Numerical Algorithms (2019) 82:69–106
https://doi.org/10.1007/s11075-018-0594-z

ORIGINAL PAPER

Investigations on several high-order ADI methods for time-space fractional diffusion equation

Shuying Zhai[1] · **Zhifeng Weng**[1] · **Xinlong Feng**[2] · **Jinyun Yuan**[3]

Received: 27 June 2017 / Accepted: 31 August 2018 / Published online: 6 October 2018

Abstract

The paper is devoted to the construction of high-precision unconditionally stable finite difference methods for solving time-space fractional diffusion equation with the Caputo fractional derivative (of order β, with $\beta \in (0, 1)$) in time and the Rimann-Liouville fractional derivatives (of order α, with $\alpha \in (1, 2]$) in space. Two kinds of difference schemes with the approximation orders $O(\tau^{2-\beta} + h^3)$ and $O(\tau^2 + h^3)$ respectively are constructed. The stability and convergence are analyzed in detail. The obtained results are illustrated numerically by some examples, and a comparative study of several high-order schemes is also carried out.

Keywords Time-space fractional diffusion equation · Caputo fractional derivative · Rimann-Liouville fractional derivative · ADI difference scheme · Stability and convergence

✉ Shuying Zhai
zhaishuying123456@163.com

Zhifeng Weng
zfwmath@163.com

Xinlong Feng
fxlmath@xju.edu.cn

Jinyun Yuan
yuanjy@gmail.com

[1] School of Mathematics Science, Huaqiao University, Quanzhou 362021, People's Republic of China

[2] College of Mathematics and Systems Science, Xinjiang University, Urumqi 830046, People's Republic of China

[3] Departamento de Matemática, Universidade Federal do Paraná, Centro Politácnico, Curitiba 81531-980, Brazil

1 Introduction

Fractional differential equations (FDEs) can be used to model many systems in various fields, such as in engineering, physics, finance hydrology, and fractional kinetics (see [1] and many references cited therein). In finance, fractional models have been used because of the relationship with certain option pricing mechanisms and heavy-tailed stochastic processes [2]. In water resources, they have been used to describe chemical and contaminant transport in heterogeneous aquifers [3]. For a recent review we refer the reader to [4]. However, most of the analytical solutions to FDEs are usually difficult to derive and always contain some infinite series even if it is luckily obtained. Therefore, the development of numerical methods for these problems has received enormous attention in recent years.

In this paper, we focus on the following time-space fractional diffusion equation:

$$\begin{cases} {}_0^C\mathcal{D}_t^\beta u(\mathbf{x},t) = \sum_{i=1}^{n} {}^{RL}\mathcal{D}_{x_i}^{\alpha_i} u(\mathbf{x},t) + f(\mathbf{x},t), & (\mathbf{x},t) \in \Omega \times (0,T], \\ u(\mathbf{x},0) = u_0(\mathbf{x}), & \mathbf{x} \in \Omega, \\ u(\mathbf{x},t) = 0, & (\mathbf{x},t) \in \partial\Omega \times (0,T], \end{cases} \tag{1}$$

where $\beta \in (0,1)$, $\alpha_i \in (1,2)$, and $\Omega = [0,1]^n (n = 1,2,3)$. The solution $u(\mathbf{x},t)$ and the source function $f(\mathbf{x},t)$ are assumed to be sufficiently smooth and have the necessary continuous partial derivatives up to certain orders. We consider up to three dimensions and hence use x, y, and z instead of x_1, x_2, and x_3 in the sequel. The derivative ${}_0^C\mathcal{D}_t^\beta u(t)$ is β-order Caputo fractional derivative defined by [7]

$${}_0^C\mathcal{D}_t^\beta u(t) = \frac{1}{\Gamma(1-\beta)} \int_0^t \frac{\partial u(s)}{\partial s} \frac{1}{(t-s)^\beta}\, ds, \qquad \beta \in (0,1),$$

and, ${}^{RL}\mathcal{D}_x^\alpha u(x)$ is α-order Rimann-Liouville fractional derivative defined by [7]

$${}^{RL}\mathcal{D}_x^\alpha u(x) = \frac{1}{\Gamma(2-\alpha)} \frac{\partial^2}{\partial x^2} \int_0^x \frac{u(\xi)}{(x-\xi)^{\alpha-1}}\, d\xi, \qquad \alpha \in (1,2).$$

Recent studies show that non-homogeneities of the medium may fundamentally alter the laws of Markov diffusion, leading to long range fluxes, and non-Gaussian, heavy-tailed profiles, and these motions may no longer obey the classical Fick's law. This phenomenon is called anomalous diffusion. The time-space fractional diffusion (1), as an important class of anomalous diffusion equations, can successfully depict the probability density of random walk models [5]. More physical interpretations of this equation can be seen in [6, 8] and references cited therein.

Study of this kind of equations can be found in [9–12] and the references therein. However, all the above works are restricted to low-dimensional problems with no more than second-order accuracy. Recently, Pang and Sun [13] applied the L_1 approximation (see, e.g., [14–18]) and the fourth-order quasi-compact difference scheme [19] for solving the 1D/2D time-space fractional diffusion equation. For the same problem, Vong et al. [20] employed the discretization formulas proposed in [21] and improved the time accuracy to second order. Nevertheless, the ADI strategy is not considered in [20].

Compared with the considerable work on the low-dimensional models, very little research has been done on the 3D time-space fractional diffusion equation. The goal of this paper is to develop some high-efficiency and high-precision ADI finite difference schemes for high-dimensional time-space fractional diffusion (1).

High-order numerical methods for approximating Riemann-Liouville fractional derivative have been considered by many authors and we mention here a few key contributions. Tian et al. [22] proposed a third-order weighted and shifted Grünwald difference (WSGD) operator for Riemann-Liouville derivative, but the resulted third-order scheme for time-dependent fractional problems will not be unconditionally stable for $\alpha \in (1, \frac{1+\sqrt{73}}{6})$. Then, they modified the method in [22] and introduced a new third-order quasi-compact finite difference scheme [23] for solving 1D/2D space fractional diffusion equations. Very recently, Ding and Li [24] presented a class of pth-order ($p \leq 6$) numerical algorithms for Riesz derivatives (with order $\alpha \in (1, 2)$) based on shifted Lubich's numerical differential formula and generating functions. But, when $p \geq 3$, the resulted p-order scheme fails to numerically solve the time-dependent space fractional diffusion equations with unconditional stability. One can easily verify it numerically or see our numerical experiments in Section 6 for more details. Then, they established another class of high-order numerical schemes [25] for Riesz derivatives (with order $\alpha \in (0, 2)$), and applied these schemes to the 1D Riesz-type turbulent diffusion equation. In this paper, we proposed a new third-order WSGD scheme for Riemann-Liouville derivatives, which is based on the idea in [22]. Compared with the above works, our new scheme is unconditional stability for time-dependent fractional problems and without extra computational cost. As a particularly interesting case, when the order of fractional derivative α equals to 1 or 2, it becomes the compact difference operators for the first- or second-order spatial derivatives with third- or fourth-order accuracy.

For the Caputo fractional derivative in time, we shall use two ways to discrete. The first way is based on the L_1 approximation, which is obtained by the standard first-order backward differentiation with the order of approximation $O(\tau^{2-\beta})$. The second is based on the significant work by Dimitrov [29], who shown that the first-order shifted Grünwald formula is the second-order approximation for the Caputo fractional derivative at some particular points. These points with superconvergence have also been used in [21, 27, 28]. For the 2D/3D cases, we also construct ADI schemes to reduce the storage requirement and the computational burden. Theoretical analyses show that the proposed schemes are unconditionally stable and convergent.

This paper is organized as follows. In Section 2, some definitions and auxiliary lemmas are given. Then, the derivation of the difference schemes **S1**, **S2**, and **S3** with order $O(\tau^{2-\beta} + h^3)$ are presented for solving the 1D/2D/3D time-space fractional diffusion equations in Sections 3 and 4 respectively. The corresponding stability and convergence are analyzed. In Section 5, three improved schemes **MS1**, **MS2**, and **MS3** with order $O(\tau^2 + h^3)$ are further investigated. And the stability and convergence analysis are given for these schemes. In Section 6, numerical experiments are performed to support the theoretical analysis and to illustrate the efficiency of the improved schemes. Finally in the last section, some conclusions are drawn.

2 Auxiliary results

We shall first give some basic definitions and recall some useful results for our use in the rest of the paper.

Definition 2.1 ([30]) Let Toeplitz matrix T_n be of the following form,

$$T_n = \begin{pmatrix} t_0 & t_{-1} & \cdots & t_{2-n} & t_{1-n} \\ t_1 & t_0 & t_{-1} & \cdots & t_{2-n} \\ \vdots & t_1 & t_0 & \ddots & \vdots \\ t_{n-2} & \cdots & \ddots & \ddots & t_{-1} \\ t_{n-1} & t_{n-2} & \cdots & t_1 & t_0. \end{pmatrix}.$$

If the diagonal elements $\{t_k\}_{k=-n+1}^{n-1}$ are the Fourier coefficients of a function $g(x)$, that is,

$$t_k = \frac{1}{2\pi}\int_{-\pi}^{\pi} g(x)e^{-Ikx}\,dx\ ,$$

then the function $g(x)$ is called the generating function of T_n, where $I = \sqrt{-1}$.

Lemma 2.1 *(Grenander-Szegö theorem [30, 31]) For the above Toeplitz matrix T_n, suppose that $g(x)$ is a 2π-periodic continuous real-valued function defined on $[-\pi, \pi]$. Denote $\lambda_{min}(T_n)$ and $\lambda_{max}(T_n)$ as the smallest and largest eigenvalues of T_n, respectively. Then, we have*

$$g_{min} \le \lambda_{min}(T_n) \le \lambda_{max}(T_n) \le g_{max}\ ,$$

where g_{min} and g_{max} denote the minimum and maximum values of $g(x)$ respectively. Moreover, if $g_{min} < g_{max}$, then all eigenvalues of T_n satisfy

$$g_{min} < \lambda(T_n) < g_{max}\ ,$$

for all $n > 0$. Furthermore, if $g_{min} \ge 0$, then T_n is positive definite.

Lemma 2.2 ([32]) *A real matrix A of order n is positive definite if and only if its symmetric part $H = \frac{A+A^T}{2}$ is positive definite; H is positive definite if and only if the eigenvalues of H are positive.*

Lemma 2.3 ([32]) *If $A \in \mathbb{C}^{n\times n}$, let $H = \frac{A+A^*}{2}$ be the Hermitian part of A, and A^* is the conjugate transpose of A. Then, for any eigenvalue λ of A, there exists*

$$\lambda_{min}(H) \le Re(\lambda) \le \lambda_{max}(H)\ ,$$

where $Re(\lambda)$ represents the real part of λ, and $\lambda_{min}(H)$ and $\lambda_{max}(H)$ are the minimum and maximum of the eigenvalues of H respectively.

Lemma 2.4 ([33]) *The matrix $A \in \mathbb{R}^{n\times n}$ is asymptotically stable if and only if there exists a symmetric and positive (or negative) definite solution $X \in \mathbb{R}^{n\times n}$ to the Lyapunov equation*

$$AX + XA^T = C,$$

where $C = C^T \in \mathbb{R}^{n\times n}$ is a negative (or positive) definite matrix. The matrix A is called asymptotically stable if all its eigenvalues have real parts in the open left half-plane, that is, $Re(\lambda(A)) < 0$.

In the following, we list some properties of Kronecker products of matrices. Here, $A \otimes B$ represents the Kroneckerproduct of A and B.

Lemma 2.5 ([33]) *Let matrices $A \in \mathbb{R}^{n\times n}$ and $B \in \mathbb{R}^{m\times m}$ have eigenvalues $\{\mu_i\}_{i=1}^n$ and $\{\nu_j\}_{j=1}^m$, respectively. Then, the mn eigenvalues of $A \otimes B$ are*

$$\mu_1\nu_1,\ \mu_1\nu_2,\ \cdots,\mu_1\nu_m,\ \mu_2\nu_1,\ \mu_2\nu_2,\ \cdots,\mu_2\nu_m,\ \mu_n\nu_1,\ \mu_n\nu_2,\ \cdots,\mu_n\nu_m.$$

Lemma 2.6 ([33]) *Let matrices $A \in \mathbb{R}^{m\times n}$, $B \in \mathbb{R}^{r\times s}$, $C \in \mathbb{R}^{n\times p}$ and $D \in \mathbb{R}^{s\times t}$. Then*

$$(A \otimes B)(C \otimes D) = AC \otimes BD (\in \mathbb{R}^{mr\times pt}).$$

Moreover, if A, $B \in \mathbb{R}^{n\times n}$, E is a unit matrix of order n, then matrices $E \otimes A$ and $B \otimes E$ commute.

Lemma 2.7 ([33]) *For all A and B, $(A \otimes B)^T = A^T \otimes B^T$.*

Lemma 2.8 ([33]) *Let A and B be two symmetric and positive semi-definite matrices, symbolized $A \geq 0$ and $B \geq 0$. Then, $A \otimes B \geq 0$.*

Lemma 2.9 ([29]) *Suppose that $\beta \in (0, 1)$, $u(t) \in C^2[0, +\infty]$, $\frac{d^3u(t)}{dt^3} \in L^1[0, +\infty)$ and $u'(0) = u''(0) = 0$. Then, for every integer p, the Caputo fractional derivative at $t_k + (p - \frac{\beta}{2})\tau$ could be approximated by the shifted Grünwald formulas*

$${}_0^C\mathcal{D}_t^\beta u\left(t_k + (p - \frac{\beta}{2})\tau\right) = \frac{1}{\tau^\beta}\sum_{l=0}^{k}\omega_l\left(u^{k+p-l} - u^0\right) + O(\tau^2).$$

An important special case of the above formula is when $p = 0$

$${}_0^C\mathcal{D}_t^\beta u\left(t_k - \frac{\beta}{2}\tau\right) = \frac{1}{\tau^\beta}\sum_{l=0}^{k}\omega_l(u^{k-l} - u^0) + O(\tau^2). \tag{2}$$

The numbers ω_l are the coefficients of the power series

$$(1 - z)^\beta = \sum_{l=0}^{\infty}\omega_l z^l$$

with

$$\omega_0 = 1, \quad \omega_l = \left(1 - \frac{1+\beta}{l}\right)\omega_{l-1} \quad for \quad l \geq 1.$$

Lemma 2.10 ([22]) *Let $u(x) \in L^1(R)$, and ${}_a^{RL}\mathcal{D}_x^{\alpha+3}u(x)$ whose Fourier transform also belongs to $L^1(R)$. Then, we have the following third-order weighted and*

shifted Grünwald difference (3-WSGD) operator for the Rimann-Liouville fractional derivative ${}_a^{RL}\mathcal{D}_x^{\alpha}u$,

$$
\begin{aligned}
{}^{RL}D^{\alpha}_{x,(p,q,r)}u(x) &= \sum_{l=0}^{\infty}\left\{\frac{\lambda_1}{h^{\alpha}}g_l^{\alpha}u\left(x-(l-p)h\right)+\frac{\lambda_2}{h^{\alpha}}g_l^{\alpha}u\left(x-(l-q)h\right)\right.\\
&\qquad\left.+\frac{\lambda_3}{h^{\alpha}}g_l^{\alpha}u\left(x-(l-r)h\right)\right\}\\
&= {}_a^{RL}\mathcal{D}_x^{\alpha}u(x_i)+O\left(h^3\right), \qquad (3)
\end{aligned}
$$

where $p, q, and r$ *are integers and* $p > q > r$, *and*

$$
\begin{cases}
\lambda_1 = \frac{12qr-(6q+6r+1)\alpha_1+3{\alpha_1}^2}{12(p-q)(p-r)},\\
\lambda_2 = \frac{12pr-(6p+6r+1)\alpha_1+3{\alpha_1}^2}{12(q-p)(q-r)},\\
\lambda_3 = \frac{12pq-(6p+6q+1)\alpha_1+3{\alpha_1}^2}{12(r-p)(r-q)},
\end{cases}
$$

and $g_l^{\alpha} = (-1)^l\binom{\alpha}{l}$ *are the coefficients of the power series of the function* $(1-z)^{\alpha}$.

Remark 2.1 Assume that $u(x) \in C^5[a,b]$ and $\frac{d^m u(x)}{dx^m}\Big|_{x=a,b} = 0$ $(m = 0, 1, \cdots, 5)$, the function $u(x)$ can be extended by zero for $x < a$ or $x > b$. Then, the extended function of $u(x)$ satisfies the conditions of Lemma 2.10. Thus, according to Lemma 2.2, the α-order Riemann-Liouville fractional derivatives of $u(x)$ at each point x can be approximated by the WSGD operators with second-order accuracy, i.e.,

$$
\begin{aligned}
{}^{RL}D^{\alpha}_{x,(p,q,r)}u(x) &= \frac{\lambda_1}{h^{\alpha}}\sum_{l=0}^{\frac{x-a}{h}+p}g_l^{\alpha}u\left(x-(l-p)h\right)+\frac{\lambda_2}{h^{\alpha}}\sum_{l=0}^{\frac{x-a}{h}+q}g_l^{\alpha}u\left(x-(l-q)h\right)\\
&\quad+\frac{\lambda_3}{h^{\alpha}}\sum_{l=0}^{\frac{x-a}{h}+r}g_l^{\alpha}u\left(x-(l-r)h\right)\\
&= {}_a^{RL}\mathcal{D}_x^{\alpha}u(x_i)+O\left(h^3\right), \qquad (4)
\end{aligned}
$$

3 A new scheme of order $O\left(\tau^{2-\beta}+h^3\right)$ for 1D time-space fractional diffusion equation

3.1 Derivation of the difference scheme S1

In this section, we first consider the 1D time-space fractional diffusion (1). In the following, α will be written in short for α_1. Introducing a uniform mesh with the time size $\tau = \frac{T}{M}$ and the space step size $h = \frac{1}{N}$, where M and N are two positive integers. Define u_i^k as the numerical approximation to $u(x_i, t_k)$ with $x_i = ih$ and $t_k = k\tau$ for $0 \le i \le N$ and $0 \le k \le M$. Similar notation gives $f_i^k = f(x_i, t_k)$.

Assume that $u(x,t) \in \mathcal{C}^2(0,T;L^1(\Omega))$. The time-fractional derivative ${}_0^C\mathcal{D}_t^\beta u(x,t)$ at t_k is estimated by

$$\begin{aligned} {}_0^C\mathcal{D}_t^\beta u_i^k &= \frac{1}{\Gamma(1-\beta)} \sum_{l=0}^{k-1} \int_{t_l}^{t_{l+1}} \frac{\partial u(x_i,\xi)}{\partial \xi} \frac{d\xi}{(t_k-\xi)^\beta} \\ &= \frac{1}{\Gamma(1-\beta)} \sum_{l=0}^{k-1} \frac{u_i^{l+1}-u_i^l}{\tau} \int_{t_l}^{t_{l+1}} \frac{d\xi}{(t_k-\xi)^\beta} + Er_\tau^k \\ &= \frac{1}{\Gamma(2-\beta)} \sum_{l=0}^{k-1} b_l \frac{u_i^{k-l}-u_i^{k-1-l}}{\tau^\beta} + Er_\tau^k, \end{aligned} \tag{5}$$

where $b_l = (l+1)^{1-\beta} - l^{1-\beta}$, Er_τ^k is the truncation error and $|Er_\tau^k| \le C_u \tau^{2-\beta}$, and C_u is a positive constant depending on only u.

In space discretization, we choose the 3-WSGD operator in Remark 2.1 to approximate the Rimann-Liouville fractional derivative ${}^{RL}\mathcal{D}_x^\alpha u$. In fact, the 3-WSGD operator with special choice $(p,q,r) = (1,0,-1)$ was given by Tian et al. in [22]. Unfortunately, the resulting finite difference scheme for time-dependent problem is not unconditionally stable. To overcome this drawback, here, we choose $(p,q,r) = (2,1,0)$; then, we obtain

$${}^{RL}D_{x,(2,1,0)}^\alpha u(x_i,t) = \frac{1}{h^\alpha} \sum_{l=0}^{i+2} c_l^\alpha u\left(x_{i-(l-2)},t\right) = {}^{RL}\mathcal{D}_x^\alpha u(x_i,t) + O\left(h^3\right), \tag{6}$$

where

$$c_0^\alpha = \lambda_1 g_0^\alpha, \quad c_1^\alpha = \lambda_1 g_1^\alpha + \lambda_2 g_0^\alpha, \quad c_l^\alpha = \lambda_1 g_l^\alpha + \lambda_2 g_{l-1}^\alpha + \lambda_3 g_{l-2}^\alpha \quad (l \ge 2),$$

and

$$\lambda_1 = \frac{\alpha^2}{8} - \frac{7\alpha}{24}, \quad \lambda_2 = \frac{-\alpha^2}{4} + \frac{13\alpha}{12}, \quad \lambda_3 = \frac{\alpha^2}{8} - \frac{19\alpha}{24} + 1.$$

The proof in next subsection shows that this choice guarantees unconditional stability for $\alpha \in (1,2]$.

Then, combining (5) and (6), we obtain the following scheme **S1** for solving 1D problem (1).

S1:

For $k = 1, \quad i = 1,2,\cdots,N-1,$

$$u_i^1 - \tau^\beta \Gamma(2-\beta)\, {}^{RL}D_{x,(2,1,0)}^\alpha u_i^1 = u_i^0 + \tau^\beta \Gamma(2-\beta) f_i^1,$$

and for $k = 2,3,\cdots,M, \quad i = 1,2,\cdots,N-1,$

$$u_i^k - \tau^\beta \Gamma(2-\beta)\, {}^{RL}D_{x,(2,1,0)}^\alpha u_i^k = u_i^{k-1} - \sum_{l=1}^{k-1} b_l \left(u_i^{k-l} - u_i^{k-1-l}\right) + \tau^\beta \Gamma(2-\beta) f_i^k,$$

where $u_{N+1}^k = \hat{u}(x_{N+1},t_k) = 0$ is given by Remark 2.1.

Remark 3.1 Specially, for α=1 or 2, scheme (6) can be respectively reduced to the compact difference operators for the first/second-order spatial derivatives with third/fourth-order accuracy, i.e.,

$$\begin{aligned} {}^{RL}D^{1}_{x,(2,1,0)}u(x) &= \frac{1}{6h}\left(-u(x+2h)+6u(x+h)-3u(x)-2u(x-h)\right) \\ &= u'(x)+O(h^3). \end{aligned}$$

and

$$\begin{aligned} {}^{RL}D^{2}_{x,(2,1,0)}u(x) &= \frac{1}{12h^2}\left(-u(x+2h)+16u(x+h)-30u(x)\right. \\ &\qquad \left.+16u(x-h)-u(x-2h)\right) \\ &= u''(x)+O\left(h^4\right). \end{aligned}$$

Inspired by the results in the two extreme cases α=1 and 2, it is reasonable to conjecture that the accuracy of scheme (6) may depend on α. Our numerical tests in Section 6 illustrate that scheme (6) can yield a spatial approximation order close to $2+\alpha$ in some cases (e.g., polynomial solutions), which verifies the conjecture.

3.2 Analysis of the difference scheme S1

In this subsection, stability and convergence analysis of scheme **S1** are discussed by mathematical induction. We will first prove the following useful result.

Lemma 3.1 *Let matrix C^{α} be of the following form,*

$$C^{\alpha}=\begin{pmatrix} c_2^{\alpha} & c_1^{\alpha} & c_0^{\alpha} & 0 & \dots & 0 & 0 \\ c_3^{\alpha} & c_2^{\alpha} & c_1^{\alpha} & c_0^{\alpha} & \dots & 0 & 0 \\ \vdots & \vdots & \vdots & \vdots & \ddots & \vdots & \vdots \\ c_{N-1}^{\alpha} & c_{N-2}^{\alpha} & c_{N-3}^{\alpha} & c_{N-4}^{\alpha} & \dots & c_2^{\alpha} & c_1^{\alpha} \\ c_N^{\alpha} & c_{N-1}^{\alpha} & c_{N-2}^{\alpha} & c_{N-3}^{\alpha} & \dots & c_3^{\alpha} & c_2^{\alpha} \end{pmatrix}, \tag{7}$$

where the diagonals $\{c_i^{\alpha}\}_{i=0}^{N}$ are the coefficients given in (6). Then, C^{α} is negative definite matrix whose eigenvalues are with negative real part for $\alpha\in(1,2]$.

Proof Let $H=\frac{C^{\alpha}+(C^{\alpha})^T}{2}$, the symmetric part of C^{α}. The generating functions of C^{α} and $(C^{\alpha})^T$ are

$$g_{C^{\alpha}}(x)=\sum_{i=0}^{\infty}c_i^{\alpha}e^{I(i-2)x}, \qquad g_{(C^{\alpha})^T}(x)=\sum_{i=0}^{\infty}c_i^{\alpha}e^{-I(i-2)x},$$

respectively.

Then, $g(\alpha;x)=\frac{g_{C^{\alpha}}(x)+g_{(C^{\alpha})^T}(x)}{2}$ is the generating function of H, and $g(\alpha;x)$ is a periodic continuous real-valued function on $[-\pi,\pi]$ since $g_{C^{\alpha}}(x)$ and $g_{(C^{\alpha})^T}(x)$

are mutually conjugated. With the corresponding coefficients c_i^α given by (6), we have

$$\begin{aligned} g(\alpha; x) &= \frac{1}{2}\left(\sum_{i=0}^{\infty} c_i^\alpha e^{I(i-2)x} + \sum_{i=0}^{\infty} c_i^\alpha e^{-I(i-2)x}\right) \\ &= \frac{1}{2}\left(\lambda_1 e^{-2Ix} + \lambda_2 e^{-Ix} + \lambda_3\right)\sum_{i=0}^{\infty} g_i^\alpha e^{Iix} \\ &\quad + \frac{1}{2}\left(\lambda_1 e^{2Ix} + \lambda_2 e^{Ix} + \lambda_3\right)\sum_{i=0}^{\infty} g_i^\alpha e^{-Iix} \\ &= \frac{\lambda_1 e^{-2Ix} + \lambda_2 e^{-Ix} + \lambda_3}{2}\left(1 - e^{Ix}\right)^\alpha \\ &\quad + \frac{\lambda_1 e^{2Ix} + \lambda_2 e^{Ix} + \lambda_3}{2}\left(1 - e^{-Ix}\right)^\alpha \\ &= \left(2\sin\left(\frac{x}{2}\right)\right)^\alpha \left[\lambda_1 \cos\left(\frac{\alpha(x-\pi)}{2} - 2x\right) + \lambda_2 \cos\left(\frac{\alpha(x-\pi)}{2} - x\right)\right. \\ &\qquad \left. + \lambda_3 \cos\left(\frac{\alpha(x-\pi)}{2}\right)\right]. \end{aligned}$$

Since $g(\alpha; x)$ is a real-valued and even function, we just consider its principal value on $[0, \pi]$. By the formula

$$e^{Ix} = \cos(x) + I\sin(x),$$

we obtain

$$\begin{aligned} g(\alpha; x) &= \left(2\sin\left(\frac{x}{2}\right)\right)^\alpha \left[\lambda_1 \cos\left(\frac{\alpha(x-\pi)}{2} - 2x\right) + \lambda_2 \cos\left(\frac{\alpha(x-\pi)}{2} - x\right)\right. \\ &\qquad \left. + \lambda_3 \cos\left(\frac{\alpha(x-\pi)}{2}\right)\right]. \end{aligned}$$

Denoting

$$h(\alpha; x) = \lambda_1 \cos\left(\frac{\alpha(x-\pi)}{2} - 2x\right) + \lambda_2 \cos\left(\frac{\alpha(x-\pi)}{2} - x\right) + \lambda_3 \cos\left(\frac{\alpha(x-\pi)}{2}\right)$$

Since $h(\alpha; x)$ decreases with respect to α (please see Appendix), thus

$$\begin{aligned} g(\alpha; x) &\le \left(2\sin\left(\frac{x}{2}\right)\right)^\alpha h(1; x) \\ &= \left(2\sin\left(\frac{x}{2}\right)\right)^\alpha \left[\frac{1}{3}\cos^2\left(\frac{x}{2}\right)\sin\left(\frac{x}{2}\right) + \frac{1}{6}\cos(x)\sin\left(\frac{x}{2}\right) - \frac{1}{2}\sin\left(\frac{x}{2}\right)\right] \\ &\le 0. \end{aligned}$$

By Lemmas 2.1 and 2.3, we get $Re(\lambda_{C^\alpha}) < 0$ for $\alpha \in (1, 2]$.

From above discussions and Lemma 2.1, we know that, for $\alpha \in (1, 2]$, the matrix $\frac{C^\alpha + (C^\alpha)^T}{2}$ is negative definite, which implies matrix C^α is negative definite by Lemma 2.2. □

From Lemma 3.1, we know that C^α is a negative definite matrix; thus, $\left(E - \frac{\tau^\beta \Gamma(2-\beta)}{h^\alpha} C^\alpha\right)$ is a positive definite matrix (where E is the identity matrix of order $(N-1)$). Then, we further have the following lemma.

Lemma 3.2 *Let C^α be defined in (7), then*

$$\| \left(E - \frac{\tau^\beta \Gamma(2-\beta)}{h^\alpha} C^\alpha\right)^{-1} \|_2 < 1.$$

where $\| \cdot \|_2$ denotes the L^2-norm (spectral norm).

Proof For convenience of writing, we define

$$D^\alpha = \frac{\tau^\beta \Gamma(2-\beta)}{h^\alpha} C^\alpha.$$

From Lemma 3.1, we know that $D^\alpha + (D^\alpha)^T$ is a negative definite and symmetric matrix. Then, for any $v = (v_1, v_2, \cdots, v_{N-1})^T \in R^{N-1}$, we obtain that

$$v^T v < v^T \left(E - (D^\alpha)^T\right)\left(E - D^\alpha\right) v.$$

Substituting v and v^T by $(E - D^\alpha)^{-1} v$ and $v^T \left(E - (D^\alpha)^T\right)^{-1}$, respectively, for any $v \in R^{N-1}$, we get

$$v^T \left(E - (D^\alpha)^T\right)^{-1} \left(E - D^\alpha\right)^{-1} v < v^T v.$$

Thus, it leads to

$$\| (E - D^\alpha)^{-1} \|_2 = \max_{v \neq 0} \frac{v^T \left(E - (D^\alpha)^T\right)^{-1} (E - D^\alpha)^{-1} v}{v^T v} < 1. \quad \square$$

Now, we consider the stability of the scheme **S1**. Without lose of generality, we consider the case $f(x,t) = 0$. Let

$$U^k = (u_1^k, u_2^k, \ldots, u_{N-1}^k)^T, \quad k = 0, \ldots, M. \tag{8}$$

$\square$

Theorem 3.1 *The fully discrete scheme **S1** is unconditionally stable in the sense that for all $h > 0$ and $\tau > 0$, it holds*

$$\| U^k \|_2 < \| U^0 \|_2, \quad k = 1, \ldots, M,$$

where $\| \cdot \|_2$ stands for the discrete L^2-norm.

Proof When $k = 1$, the expression of scheme **S1** is

$$\left(E - \frac{\tau^\beta \Gamma(2-\beta)}{h^\alpha} C^\alpha\right) U^1 = U^0.$$

Since $E - \frac{\tau^\beta \Gamma(2-\beta)}{h^\alpha} C^\alpha$ is a positive definite matrix, then we have

$$U^1 = \left(E - \frac{\tau^\beta \Gamma(2-\beta)}{h^\alpha} C^\alpha\right)^{-1} U^0,$$

Taking the L^2-norm on both sides, we have that

$$\| U^1 \|_2 \leq \| \left(E - \frac{\tau^\beta \Gamma(2-\beta)}{h^\alpha} C^\alpha\right)^{-1} \|_2 \| U^0 \|_2 < \| U^0 \|_2,$$

where Lemma 3.2 shows that $\| \left(E - \frac{\tau^\beta \Gamma(2-\beta)}{h^\alpha} C^\alpha\right)^{-1} \|_2 < 1$.

Using the mathematical induction, we suppose that

$$||U^k||_2 < ||U^0||_2, \qquad k = 1, \ldots, L. \tag{9}$$

to prove $||U^{L+1}||_2 < ||U^0||_2$.

For $k = L+1$, scheme **S1** can be written in the form of

$$\begin{aligned}\left(E - \frac{\tau^\beta \Gamma(2-\beta)}{h^\alpha} C^\alpha\right) U^{L+1} &= U^L - \sum_{l=1}^{L} b_l \left(U^{L-l} - U^{L-1-l}\right) \\ &= \sum_{l=1}^{L} (b_{l-1} - b_l) U^{L+1-l} + b_L U^0.\end{aligned}$$

Mergering similar items and acting $\left(E - \frac{\tau^\beta \Gamma(2-\beta)}{h^\alpha} C^\alpha\right)^{-1}$ on both sides, we obtain that

$$U^{L+1} = \left(E - \frac{\tau^\beta \Gamma(2-\beta)}{h^\alpha} C^\alpha\right)^{-1} \left(\sum_{l=1}^{L} (b_{l-1} - b_l) U^{L+1-l} + b_L U^0\right).$$

Taking the L^2-norm on both sides and using Lemma 3.2 and (9), we have that

$$\begin{aligned}||U^{L+1}||_2 &\leq \sum_{l=1}^{L} (b_{l-1} - b_l) || \left(E - \frac{\tau^\beta \Gamma(2-\beta)}{h^\alpha} C^\alpha\right)^{-1} ||_2 ||U^{L+1-l}||_2 \\ &\quad + b_L || \left(E - \frac{\tau^\beta \Gamma(2-\beta)}{h^\alpha} C^\alpha\right)^{-1} ||_2 ||U^0||_2 \\ &< \sum_{l=1}^{L} (b_{l-1} - b_l) ||U^{L+1-l}||_2 + b_L ||U^0||_2 \\ &< \sum_{l=1}^{L} (b_{l-1} - b_l) ||U^0||_2 + b_L ||U^0||_2 = ||U^0||_2,\end{aligned}$$

The proof is completed. □

Denote

$$e_i^k = u(x_i, t_k) - u_i^k, \quad 0 < i < N, 0 < k \leq M.$$

Next we will present the main convergence result.

Theorem 3.2 *Suppose that* $u(x,t) \in C^2\left(0,T;C^5(a,b)\right)$ *and* $\left.\frac{\partial^m u(x,t)}{\partial x^m}\right|_{x=a,\ b} = 0$ $(m = 0, 1, \cdots, 5)$. *If* $u(x_i,t_k)$ *and* u_i^k *are respectively the exact solution of problem (4) and the difference solution of the scheme* ***S1*** *respectively at grid point* (x_i,t_k). *Then, there exists a positive constant* ψ *such that*

$$\| e^k \|_2 \le b_{k-1}^{-1}\psi\left(\tau^2+\tau^\beta h^3\right), \quad k=1,2,\ldots,M, \tag{10}$$

where ψ *denotes a positive constant and is independent of* τ *and* h.

Proof By **S1**, if $k=0$,

$$e^1 = \left(E - \frac{\tau^\beta\Gamma(2-\beta)}{h^\alpha}C^\alpha\right)^{-1} e^0 + \tau^\beta R^1,$$

where R^1 is the truncation error and $|R^1| \le \psi\left(\tau^{2-\beta}+h^3\right)$.

Together with

$$e^0 = 0$$

and $\| \left(E - \frac{\tau^\beta\Gamma(2-\beta)}{h^\alpha}C^\alpha\right)^{-1} \|_2 < 1$ in Lemma 3.2, then the above equation becomes as

$$\| e^1 \|_2 \le \psi\left(\tau^2+\tau^\beta h^3\right) = \psi b_0^{-1}\left(\tau^2+\tau^\beta h^3\right).$$

Let us use mathematical induction method to prove the desired result. Suppose that $\| e^k \|_2 \le \psi b_{k-1}^{-1}\left(\tau^2+\tau^\beta h^3\right)$ for all $k=1,\ldots,L$. Then, we shall prove that it holds also for $k=L+1$. By **S1**, we have

$$e^{L+1} = \left(E - \frac{\tau^\beta\Gamma(2-\beta)}{h^\alpha}C^\alpha\right)^{-1}\sum_{l=1}^{L}(b_{l-1}-b_l)\,e^{L+1-l} + \tau^\beta R^{L+1},$$

where R^{L+1} is the truncation error at t_{L+1}.

Noting that $0 < b_l^{-1} < b_L^{-1}$, $l=1,2,\ldots,L-1$, and $\| \left(E - \frac{\tau^\beta\Gamma(2-\beta)}{h^{\alpha_1}}C^\alpha\right)^{-1} \|_2 < 1$, and $|R^{L+1}| \le \psi\left(\tau^{2-\beta}+h^3\right)$, we have

$$\begin{aligned}
\| e^{L+1} \|_2 &< \sum_{l=1}^{L}(b_{l-1}-b_l)\,\| e^{L+1-l} \|_2 + \tau^\beta|R^{L+1}| \\
&< \left(\sum_{l=1}^{L}(b_{l-1}-b_l)b_{L-l}^{-1}+1\right)\psi\left(\tau^2+\tau^\beta h^3\right) \\
&< b_L^{-1}\left(\sum_{l=1}^{L}(b_{l-1}-b_l)+b_L\right)\psi\left(\tau^2+\tau^\beta h^3\right) \\
&= b_L^{-1}\psi\left(\tau^2+\tau^\beta h^3\right).
\end{aligned}$$

Hence, the estimation (10) is proved. □

Since

$$k^{-\beta}b_{k-1}^{-1}=\frac{k^{-\beta}}{k^{1-\beta}-(k-1)^{1-\beta}}=\frac{k^{-1}}{1-(1-k^{-1})^{1-\beta}}\longrightarrow\frac{1}{1-\beta},\ \text{as } k\longrightarrow\infty,$$

there exists a positive constant C such that $k^{-\beta}b_{k-1}^{-1}<\frac{C}{1-\beta}$.

Thus, we have, for all l such that $l\tau\le T$,

$$\parallel e^k\parallel_2\le b_{k-1}^{-1}\psi\left(\tau^2+\tau^\beta h^3\right)\le\frac{C}{1-\beta}\psi k^\beta\left(\tau^2+\tau^\beta h^3\right)\le\phi T^\beta\left(\tau^{2-\beta}+h^3\right),$$

where $\phi=\frac{C}{1-\beta}\psi$ is a positive constant and independent of τ and h.

Theorem 3.3 *Suppose that* $u(x,t)\in C^2\left(0,T;C^5(a,b)\right)$ *and* $\frac{\partial^m u(x,t)}{\partial x^m}\Big|_{x=a,b}=0$ $(m=0,1,\cdots,5)$. *If* $u(x_i,t_k)$ *and* u_i^k *are respectively the exact solution of (1) and the difference solution of the scheme* ***S1*** *at grid point* (x_i,t_k), *then there exists a positive constant* ϕ, *such that*

$$\parallel e^k\parallel_2\le\phi T^\beta\left(\tau^{2-\beta}+h^3\right),\quad k=1,2,\ldots,M.$$

4 Two new ADI difference schemes of order $O\left(\tau^{2-\beta}+h^3\right)$ for 2D/3D time-space fractional diffusion equations

4.1 Derivation of the difference scheme S2

In this subsection, we consider the 2D time-space fractional diffusion (1). Define u_{ij}^k as the numerical approximation to $u(x_i,y_j,t_k)$, with $x_i=ih$, $y_j=jh$, and $t_k=k\tau$. Similar notation gives $f_{ij}^k=f(x_i,y_j,t_k)$. The definitions of τ and h are the same as ones mentioned in Section 3. In this subsection, u^k and f^k will be respectively written in short for u_{ij}^k and f_{ij}^k if there is no confusion about these notations.

Similar to the process of dealing with the 1D case, the high-order difference scheme for solving 2D problem (1) can be constructed as follows

$$u_{ij}^k-\tau^\beta\Gamma(2-\beta)\left({}^{RL}D_{x,(2,1,0)}^{\alpha_1}+{}^{RL}D_{y,(2,1,0)}^{\alpha_2}\right)u_{ij}^k=u_{ij}^{k-1}+F_{ij}^k,\tag{11}$$

where

$$F_{ij}^k=\begin{cases}\tau^\beta\Gamma(2-\beta)f_{ij}^k, & k=1,\\ -\sum\limits_{l=1}^{k-1}b_l\left(u_{ij}^{k-l}-u_{ij}^{k-1-l}\right)+\tau^\beta\Gamma(2-\beta)f_{ij}^k, & 2\le k\le M.\end{cases}$$

and the values $u_{N+1,j}^k=u_{i,N+1}^k=0$, which can be obtained from Remark 2.1.

Note that at each time step, scheme (11) requires solving a very large non-sparse linear system of equations with $(N-1)^2$ unknowns, which is computationally

intensive. The problem becomes more computationally demanding as finer grid resolutions. A preferable choice is the use of ADI methods, where the difference equations are specified and solved in one direction at a time. Following, we introduce an additional perturbation error and rewrite scheme (11) in a directional separation product form.

For convenience of writing, we define

$$L^{\beta}_{\alpha_1} = \tau^{\beta}\Gamma(2-\beta)^{RL}D^{\alpha_1}_{x,(2,1,0)} \quad \text{and} \quad L^{\beta}_{\alpha_2} = \tau^{\beta}\Gamma(2-\beta)^{RL}D^{\alpha_2}_{y,(2,1,0)}. \tag{12}$$

Then, a simple perturbation error is given

$$L^{\beta}_{\alpha_1}L^{\beta}_{\alpha_2}\left(u^k - 2u^{k-1} + u^{k-2}\right) = O\left(\tau^{2+2\beta}\right), \quad k \geq 2 \tag{13}$$

Adding this term onto the right-hand side of (11). After rearranging the terms, an ADI scheme for $k \geq 2$ is obtained

$$\textbf{S2:} \quad \left(I - L^{\beta}_{\alpha_1}\right)\left(I - L^{\beta}_{\alpha_2}\right)u^k = u^{k-1} + F^k + L^{\beta}_{\alpha_1}L^{\beta}_{\alpha_2}\left(2u^{k-1} - u^{k-2}\right)$$

with obtaining u^1 by solving

$$\left(I - L^{\beta}_{\alpha_1}\right)\left(I - L^{\beta}_{\alpha_2}\right)u^1 = u^0 + F^1 + L^{\beta}_{\alpha_1}L^{\beta}_{\alpha_2}u^0, \tag{14}$$

where $u^k_{i,N+1} = 0$ and $u^k_{N+1,j} = 0$.

Computationally, the ADI method for the above form is set up and solved by the following iterative schemes. Introducing one intermediate variable u^*, schemes (14) and **S2** can be solved in two steps as

$$\begin{cases} \left(I - L^{\beta}_{\alpha_1}\right)u^* = u^0 + F^1 + L^{\beta}_{\alpha_1}L^{\beta}_{\alpha_2}u^0, & \text{(15a)} \\ \left(I - L^{\beta}_{\alpha_2}\right)u^1 = u^*, & \text{(15b)} \end{cases}$$

and

$$\begin{cases} \left(I - L^{\beta}_{\alpha_1}\right)u^* = u^{k-1} + F^k + L^{\beta}_{\alpha_1}L^{\beta}_{\alpha_2}\left(2u^{k-1} - u^{k-2}\right), & \text{(16a)} \\ \left(I - L^{\beta}_{\alpha_2}\right)u^k = u^*. & \text{(16b)} \end{cases}$$

Here, the values of u^* on the boundary are easily obtained from (15b) and (16b), respectively.

Remark 4.1 Since $1 + \beta > 2 - \beta$ for $\beta \in [\frac{1}{2}, 1)$, it seems that we can use

$$L^{\beta}_{\alpha_1}L^{\beta}_{\alpha_2}\left(u^k - u^{k-1}\right) = O\left(\tau^{1+2\beta}\right), \quad k \geq 1. \tag{17}$$

instead of (13). Although the resulted schemes from both perturbation errors have the similar truncation errors, numerical experiments in [36] show that (13) is much

better than (17), regardless of the value of β. We would like to comment the fact that in most ADI methods, the splitting terms are of the same or higher order as the truncation error terms associated with the underlying numerical methods. Thus, the asymptotic rates of convergence for an ADI method should be of the same order in the spatial and temporal discretization parameters as those for its associated underlying method. However,at practical levels of discretization, the actual errors associated with an ADI method can be much larger than that for the underlying method. We will further illustrate this phenomenon by numerical experiments in Section 6.

In some cases, the splitting error totally dominates the error for the AD procedure, which motivates us to reduce the splitting error. Although ADI methods [15, 26] have been widely used for solving fractional differential equations, few of them are considered from this point of view.

4.2 Stability and convergence analysis of S2

In this subsection, we shall demonstrate the stability and convergence of scheme **S2**.

Lemma 4.1 *Let* $C^{\alpha_1,\alpha_2} = \frac{1}{h^{\alpha_1}} E \otimes C^{\alpha_1} + \frac{1}{h^{\alpha_2}} C^{\alpha_2} \otimes E$, *where* $E \in \mathbb{R}^{(N-1)\times(N-1)}$ *is a unit matrix, and* $C^{\alpha_1}, C^{\alpha_2} \in \mathbb{R}^{(N-1)\times(N-1)}$ *have the same form as* (7). *Then,* C^{α_1,α_2} *is asymptotically stable.*

Proof By Lemma 2.4 and Lemma 3.1, we know that C^{α_1} and C^{α_2} are asymptotically stable. This means that there exist symmetric matrices X_1, X_2, B_1, $B_2 \in \mathbb{R}^{(N-1)\times(N-1)}$ such that

$$C^{\alpha_1} X_1 + X_1 (C^{\alpha_1})^T = B_1, \quad C^{\alpha_2} X_2 + X_2 (C^{\alpha_2})^T = B_2.$$

Denoting symmetric and positive matrix $X = X_2 \otimes X_1$, from Lemma 2.6 and Lemma 2.7, we have

$$\begin{aligned}
& C^{\alpha_1,\alpha_2} X + X (C^{\alpha_1,\alpha_2})^T \\
= & \frac{1}{h^{\alpha_1}} (E \otimes C^{\alpha_1})(X_2 \otimes X_1) + \frac{1}{h^{\alpha_2}} (C^{\alpha_2} \otimes E)(X_2 \otimes X_1) \\
& + \frac{1}{h^{\alpha_1}} (X_2 \otimes X_1)(E \otimes C^{\alpha_1})^T + \frac{1}{h^{\alpha_2}} (X_2 \otimes X_1)(C^{\alpha_2} \otimes E)^T \\
= & \frac{1}{h^{\alpha_1}} X_2 \otimes (C^{\alpha_1} X_1) + \frac{1}{h^{\alpha_2}} (C^{\alpha_2} X_2) \otimes X_1 + \frac{1}{h^{\alpha_1}} X_2 \otimes \left(X_1 (C^{\alpha_1})^T \right) \\
& + \frac{1}{h^{\alpha_2}} \left(X_2 (C^{\alpha_2})^T \right) \otimes X_1 \\
= & \frac{1}{h^{\alpha_1}} X_2 \otimes \left(C^{\alpha_1} X_1 + X_1 (C^{\alpha_1})^T \right) + \frac{1}{h^{\alpha_2}} \left(C^{\alpha_2} X_2 + X_2 (C^{\alpha_2})^T \right) \otimes X_1 \\
= & \frac{1}{h^{\alpha_1}} X_2 \otimes B_1 + \frac{1}{h^{\alpha_2}} B_2 \otimes X_1.
\end{aligned}$$

Then, for any $\phi=(\phi_1,\phi_2,\cdots,\phi_{N-1})^T\in\mathbb{R}^{N-1}\setminus 0$ and $\varphi=(\varphi_1,\varphi_2,\cdots,\varphi_{N-1})^T\in\mathbb{R}^{N-1}\setminus 0$, it follows from Lemmas 2.6–2.8 that

$$\begin{aligned}
&(\phi\otimes\varphi)^T\left(\frac{1}{h^{\alpha_1}}X_2\otimes B_1+\frac{1}{h^{\alpha_2}}B_2\otimes X_1\right)(\phi\otimes\varphi)\\
=&\ \frac{1}{h^{\alpha_1}}(\phi\otimes\varphi)^T(X_2\otimes B_1)(\phi\otimes\varphi)+\frac{1}{h^{\alpha_2}}(\phi\otimes\varphi)^T(B_2\otimes X_1)(\phi\otimes\varphi)\\
=&\ \frac{1}{h^{\alpha_1}}[(\phi^TX_2)\otimes(\varphi^TB_1)](\phi\otimes\varphi)+\frac{1}{h^{\alpha_2}}[(\phi^TB_2)\otimes(\varphi^TX_1)](\phi\otimes\varphi)\\
=&\ \frac{1}{h^{\alpha_1}}(\phi^TX_2\phi)\otimes(\varphi^TB_1\varphi)+\frac{1}{h^{\alpha_2}}(\phi^TB_2\phi)\otimes(\varphi^TX_1\varphi)\\
<&\ 0,
\end{aligned}$$

which means that $\frac{1}{h^{\alpha_1}}X_2\otimes B_1+\frac{1}{h^{\alpha_2}}B_2\otimes X_1$ is a negative matrix. Moreover,

$$\begin{aligned}
\left(\frac{1}{h^{\alpha_1}}X_2\otimes B_1+\frac{1}{h^{\alpha_2}}B_2\otimes X_1\right)^T&=\frac{1}{h^{\alpha_1}}X_2^T\otimes B_1^T+\frac{1}{h^{\alpha_2}}B_2^T\otimes X_1^T\\
&=\frac{1}{h^{\alpha_1}}X_2\otimes B_1+\frac{1}{h^{\alpha_2}}B_2\otimes X_1.
\end{aligned}$$

Then, it yields from Lemma 2.4 that C^{α_1,α_2} is asymptotically stable. □

Since schemes (11) and **S2** are equivalent, now we only consider the stability of scheme (11). Without lose of generality, we consider the case $f(x,y,t)=0$. We express grid function u_{ij}^k in the vector form as

$$\begin{aligned}
U^k=\Big(&u_{1,1}^k,u_{2,1}^k,\ldots,u_{N-1,1}^k,u_{1,2}^k,u_{2,2}^k,\ldots,u_{N-1,2}^k,\cdots,\\
&u_{1,N-1}^k,u_{2,N-1}^k,\ldots,u_{N-1,N-1}^k\Big)^T.
\end{aligned}\tag{18}$$

Theorem 4.1 *The fully discrete scheme of (11) is unconditionally stable in the sense that for all $h>0$ and $\tau>0$, it holds*

$$||U^k||_2<||U^0||_2,\quad k=1,\ldots,M.$$

Proof Expressing the equation system of (11) in matrix form

$$\left(E-\tau^\beta\Gamma(2-\beta)C^{\alpha_1,\alpha_2}\right)U^k=U^{k-1}-\sum_{l=1}^{k-1}b_l\left(U^{k-l}-U^{k-1-l}\right),$$

where $E\in\mathbb{R}^{(N-1)^2\times(N-1)^2}$ is a unit matrix.

Note that matrices C^{α_1} and C^{α_2} are negative definite by Lemma 3.1. Hence, based on Lemma 4.1 and Lemma 2.4, C^{α_1,α_2} is also negative definite which follows that $\left(E-\tau^\beta\Gamma(2-\beta)C^{\alpha_1,\alpha_2}\right)$ is positive definite. On the other hand, based on Lemma 3.1, it is easy to show that $\|\ (E-\tau^\beta\Gamma(2-\beta)C^{\alpha_1,\alpha_2})^{-1}\ \|_2<1$. For the rest of the proof, the reader is referred to Theorem 3.1. The concrete process is omitted here. □

Denote

$$e_{ij}^k = u(x_i, y_j, t_k) - u_{ij}^k, \quad 0 < i, j < N, 0 < k \le M.$$

By the similar approach used in Theorem 3.2, we can obtain the following convergence result for (11).

Theorem 4.2 *Suppose that* $u(x, y, t) \in C^2\left(0, T; C^5(\Omega)\right)$ *and* $\frac{\partial^m u(\boldsymbol{x},t)}{\partial \boldsymbol{x}^m}\Big|_{\boldsymbol{x}\in\partial\Omega} = 0$ $(m = 0, 1, \cdots, 5)$. *If* $u(x_i, y_j, t_k)$ *and* u_{ij}^k *are respectively the exact solution of (1) and the difference solution of scheme (11) at grid point* (x_i, y_j, t_k), *then there exists positive constant* ϕ *such that*

$$\| e^k \|_2 \le \phi T^\beta \left(\tau^{2-\beta} + h^3\right), \quad k = 1, 2, \ldots, M.$$

4.3 Derivation of the difference scheme S3

In this subsection, we consider the 3D time-space fractional diffusion (1).

For convenience of writing, we define

$$L_{\alpha_3}^\beta = \tau^\beta \Gamma(2-\beta)\, {}^{RL}D_{z,(2,1,0)}^{\alpha_3}, \quad L_{\text{err}} = L_{\alpha_1}^\beta L_{\alpha_2}^\beta + L_{\alpha_1}^\beta L_{\alpha_3}^\beta + L_{\alpha_2}^\beta L_{\alpha_3}^\beta - L_{\alpha_1}^\beta L_{\alpha_2}^\beta L_{\alpha_3}^\beta,$$

where the operators $L_{\alpha_1}^\beta$ and $L_{\alpha_2}^\beta$ are defined by (12).

Similar to the process of dealing with the 2D case, we can directly obtain the following difference scheme for 3D problem (1)

$$u^k - \left(L_{\alpha_1}^\beta + L_{\alpha_2}^\beta + L_{\alpha_3}^\beta\right) u^k = u^{k-1} + F^k,$$

and the corresponding ADI difference scheme

$$\textbf{S3:} \quad \left(I - L_{\alpha_1}^\beta\right)\left(I - L_{\alpha_2}^\beta\right)\left(I - L_{\alpha_3}^\beta\right) u^k = u^{k-1} + F^k + L_{\text{err}}\left(2u^{k-1} - u^{k-2}\right)$$

with obtaining u^1 by solving

$$\left(I - L_{\alpha_1}^\beta\right)\left(I - L_{\alpha_2}^\beta\right)\left(I - L_{\alpha_3}^\beta\right) u^1 = u^0 + F^1 + L_{\text{err}} u^0, \quad \beta \in (0, 1),$$

where

$$F^k = \begin{cases} \tau^\beta \Gamma(2-\beta) f^k, & k = 1, \\ -\sum\limits_{l=1}^{k-1} b_l \left(u^{k-l} - u^{k-1-l}\right) + \tau^\beta \Gamma(2-\beta) f^k, & 2 \le k \le M. \end{cases}$$

and $u^k = u_{ijl}^k$, $f^k = f_{ijl}^k = f(x_i, y_j, z_l, t_k)$ $(x_i{=}ih,\ y_j{=}jh,\ z_l{=}lh,\ t_k{=}k\tau)$, and from Remark 2.1, we know that the values $u_{N+1,j,l}^k{=}u_{i,N+1,l}^k{=}u_{i,j,N+1}^k = 0$.

Now, we directly give the stability and convergence for the scheme **S3**, which can be obtained by using the similar idea as the 2D case. First, expressing grid function u_{ijl}^k in the vector form as

$$\begin{aligned} U^k = \Big(&u_{1,1,1}^k, u_{2,1,1}^k, \cdots, u_{N-1,1,1}^k, \ \cdots, \ u_{1,2,1}^k, u_{2,2,1}^k, \cdots, u_{N-1,2,1}^k, \\ &\cdots, \ u_{1,N-1,1}^k, u_{2,N-1,1}^k, \cdots, u_{N-1,N-1,1}^k, \cdots, \\ &u_{1,N-1,N-1}^k, u_{2,N-1,N-1}^k, \cdots, u_{N-1,N-1,N-1}^k\Big)^T, \end{aligned} \tag{19}$$

and denoting

$$e_{ijl}^k = u(x_i, y_j, z_l, t_k) - u_{ijl}^k, \quad 0 < i, j, l < N, 0 < k \le M.$$

Then, we have the following results.

Theorem 4.3 *The fully discrete scheme of **S3** is unconditionally stable in the sense that for all $h > 0$ and $\tau > 0$, it holds*

$$||U^k||_2 < ||U^0||_2, \quad k = 1, \ldots, M.$$

Theorem 4.4 *Suppose that $u(x, y, z, t) \in C^2\left(0, T; C^5(\Omega)\right)$ and $\frac{\partial^m u(\boldsymbol{x},t)}{\partial \boldsymbol{x}^m}\Big|_{\boldsymbol{x}\in\partial\Omega} = 0$ $(m = 0, 1, \cdots, 5)$. If $u(x_i, y_j, z_l, t_k)$ and u_{ijl}^k are respectively the exact solution of problem (1) and the difference solution of scheme **S3** at grid point (x_i, y_j, z_l, t_k), then there exists positive constant ϕ such that*

$$\| e^k \|_2 \le \phi T^\beta (\tau^{2-\beta} + h^3), \quad k = 1, 2, \ldots, M.$$

5 Three improved schemes of order $O\left(\tau^2 + h^3\right)$ for 1D/2D/3D time-space fractional diffusion equations

5.1 Derivation of the difference schemes MS1-MS3

In this section, to improve the numerical accuracy of difference schemes in time, three improved formats for 1D/2D/3D problems (1) with the approximation order $O(\tau^2 + h^3)$ are constructed. In the following, u^k will be written in short for u_i^k or u_{ij}^k or u_{ijl}^k under different circumstances if there is no confusion about the notation.

For 1D problem (1) at $(x_i, t_{k+1-\beta/2})$, it follows from (2) and (6) that

$$\frac{1}{\tau^\beta}\sum_{l=0}^{k}\omega_l\left(u^{k-l} - u^0\right) = {}^{RL}D_{x,(2,1,0)}^{\alpha} u^{k+1-\frac{\beta}{2}} + f^{k+1-\frac{\beta}{2}} + O\left(\tau^2 + h^3\right). \tag{20}$$

Note that

$$u^{k+1-\frac{\beta}{2}} = \frac{\beta}{2}u^k + \left(1 - \frac{\beta}{2}\right)u^{k+1} + O\left(\tau^2\right).$$

Substituting the above equation into (20), then multiplying (20) by τ^β and neglecting small terms, after rearranging the terms of the resulted scheme, we establish an

improved difference scheme with the approximation order $O(\tau^2 + h^3)$ for solving 1D problem (1) as follows:

$$\begin{aligned}\textbf{MS1}: \quad & u^k - \left(1 - \frac{\beta}{2}\right) \tau^\beta \, {}^{RL}D^{\alpha}_{x,(2,1,0)} u^k \\ & = \frac{\beta}{2} \tau^\beta \, {}^{RL}D^{\alpha}_{x,(2,1,0)} u^{k-1} + u^0 - \sum_{l=1}^{k} \omega_l \left(u^{k-l} - u^0\right) + \tau^\beta f^{k-\frac{\beta}{2}}.\end{aligned}$$

Let us now consider 2D/3D problems (1) at $(x_i, y_j, t_{k+1-\beta/2})$ and $(x_i, y_j, z_l, t_{k+1-\beta/2})$ respectively. Neglecting small terms, it follows from (2) and (6) that

$$\frac{1}{\tau^\beta} \sum_{l=0}^{k} \omega_l \left(u^{k-l} - u^0\right) = \left({}^{RL}D^{\alpha_1}_{x,(2,1,0)} + {}^{RL}D^{\alpha_2}_{y,(2,1,0)}\right) u^{k+1-\frac{\beta}{2}} + f^{k+1-\frac{\beta}{2}},$$

and

$$\begin{aligned}\frac{1}{\tau^\beta} \sum_{l=0}^{k} \omega_l \left(u^{k-l} - u^0\right) = & \left({}^{RL}D^{\alpha_1}_{x,(2,1,0)} + {}^{RL}D^{\alpha_2}_{y,(2,1,0)} + {}^{RL}D^{\alpha_3}_{z,(2,1,0)}\right) u^{k+1-\frac{\beta}{2}} \\ & + f^{k+1-\frac{\beta}{2}},\end{aligned}$$

Performing the same procedure as **MS1**, we further get two improved difference schemes with the approximation order $O(\tau^2 + h^3)$:

$$\begin{aligned} & u^k - \tau^\beta \left(1 - \frac{\beta}{2}\right) \left[{}^{RL}D^{\alpha_1}_{x,(2,1,0)} + {}^{RL}D^{\alpha_2}_{y,(2,1,0)} \right] u^k \\ = \; & \tau^\beta \frac{\beta}{2} \left[{}^{RL}D^{\alpha_1}_{x,(2,1,0)} + {}^{RL}D^{\alpha_2}_{y,(2,1,0)} \right] u^{k-1} + u^0 \\ & - \sum_{l=1}^{k} \omega_l \left(u^{k-l} - u^0\right) + \tau^\beta f^{k-\frac{\beta}{2}}. \end{aligned} \tag{21}$$

and

$$\begin{aligned} & u^k - \tau^\beta \left(1 - \frac{\beta}{2}\right) \left[{}^{RL}D^{\alpha_1}_{x,(2,1,0)} + {}^{RL}D^{\alpha_2}_{y,(2,1,0)} + {}^{RL}D^{\alpha_3}_{z,(2,1,0)} \right] u^k \\ = \; & \tau^\beta \frac{\beta}{2} \left[{}^{RL}D^{\alpha_1}_{x,(2,1,0)} + {}^{RL}D^{\alpha_2}_{y,(2,1,0)} + {}^{RL}D^{\alpha_3}_{z,(2,1,0)} \right] u^{k-1} + u^0 \\ & - \sum_{l=1}^{k} \omega_l \left(u^{k-l} - u^0\right) + \tau^\beta f^{k-\frac{\beta}{2}}. \end{aligned} \tag{22}$$

Furthermore, in order to obtain an effective ADI schemes for the above schemes, adding two small terms

$$\left(\frac{1-\frac{\beta}{2}}{\Gamma(2-\beta)}\right)^2 L^{\beta}_{\alpha_1} L^{\beta}_{\alpha_2}(u^k - 2u^{k-1} + u^{k-2}),$$
$$\left\{\left(\frac{1-\frac{\beta}{2}}{\Gamma(2-\beta)}\right)^2 \left[L^{\beta}_{\alpha_1} L^{\beta}_{\alpha_2} + L^{\beta}_{\alpha_1} L^{\beta}_{\alpha_3} + L^{\beta}_{\alpha_2} L^{\beta}_{\alpha_3}\right] - \left(\frac{1-\frac{\beta}{2}}{\Gamma(2-\beta)}\right)^3 L^{\beta}_{\alpha_1} L^{\beta}_{\alpha_2} L^{\beta}_{\alpha_3}\right\}$$
$$\times \left(u^k - 2u^{k-1} + u^{k-2}\right) \tag{23}$$

onto the right-hand sides of (21) and (22), respectively, we deduce that

$$\begin{aligned}
&\left(I - \frac{L^{\beta}_{\alpha_1}}{2\Gamma(1-\beta)}\right)\left(I - \frac{L^{\beta}_{\alpha_2}}{2\Gamma(1-\beta)}\right) u^k \\
\textbf{MS2}: \quad &= \frac{L^{\beta}_{\alpha_1} L^{\beta}_{\alpha_2}}{(2\Gamma(1-\beta))^2}\left(2u^{k-1} - u^{k-2}\right) + \frac{\beta}{2\Gamma(2-\beta)}\left(L^{\beta}_{\alpha_1} + L^{\beta}_{\alpha_2}\right) u^{k-1} \\
&\quad + u^0 - \sum_{l=1}^{k} \omega_l \left(u^{k-l}_{ij} - u^0\right) + \tau^{\beta} f^{k-\frac{\beta}{2}}.
\end{aligned}$$

and

$$\begin{aligned}
&\left(I - \frac{L^{\beta}_{\alpha_1}}{2\Gamma(1-\beta)}\right)\left(I - \frac{L^{\beta}_{\alpha_2}}{2\Gamma(1-\beta)}\right)\left(I - \frac{L^{\beta}_{\alpha_3}}{2\Gamma(1-\beta)}\right) u^k \\
\textbf{MS3}: \quad &= \left\{\frac{\left[L^{\beta}_{\alpha_1} L^{\beta}_{\alpha_2} + L^{\beta}_{\alpha_1} L^{\beta}_{\alpha_3} + L^{\beta}_{\alpha_2} L^{\beta}_{\alpha_3}\right]}{(2\Gamma(1-\beta))^2} - \frac{L^{\beta}_{\alpha_1} L^{\beta}_{\alpha_2} L^{\beta}_{\alpha_3}}{(2\Gamma(1-\beta))^3}\right\}\left(2u^{k-1} - u^{k-2}\right) \\
&\quad + \frac{\beta}{2\Gamma(2-\beta)}\left(L^{\beta}_{\alpha_1} + L^{\beta}_{\alpha_2} + L^{\beta}_{\alpha_3}\right) u^{k-1} + u^0 - \sum_{l=1}^{k} \omega_l \left(u^{k-l} - u^0\right) \\
&\quad + \tau^{\beta} f^{k-\frac{\beta}{2}}.
\end{aligned}$$

Here, u^1 in **MS2** and **MS3** can be obtained by using u^{k-1} instead of $2u^{k-1} - u^{k-2}$.

5.2 Stability and convergence analysis of MS1–MS3

Now, we discuss the stability and convergence of schemes **MS1**–**MS3**. Note that the discretization matrix of $\mathcal{D}_x^{\alpha_1}$ is $\frac{1}{h^{\alpha_1}} C^{\alpha_1}$. In order to simplify the notations, defining

$$\mathbf{D} = \frac{1}{h^{\alpha_1}} C^{\alpha_1}$$

offers the discretization matrix of the fractional operator $\mathcal{D}_x^{\alpha_1}$ in 1D case. Using the Kronecker tensor product notation, we can obtain the corresponding discretization matrices in 2D

$$\mathbf{D} = \frac{1}{h^{\alpha_1}} E \otimes C^{\alpha_1} + \frac{1}{h^{\alpha_2}} C^{\alpha_2} \otimes E$$

and 3D

$$\mathbf{D} = \frac{1}{h^{\alpha_1}} E \otimes E \otimes C^{\alpha_1} + \frac{1}{h^{\alpha_2}} E \otimes C^{\alpha_2} \otimes E + \frac{1}{h^{\alpha_3}} C^{\alpha_2} \otimes E \otimes E.$$

By Lemmas 2.5 and 3.1, we know $-D$ is positive definite matrix, thus

$$(-D) = (-D)^{\frac{1}{2}} (-D)^{\frac{1}{2}}.$$

Before analyzing the stability, we introduce a lemma.

Lemma 5.1 *([34]) Let $\{\omega_l\}$ be given by Lemma 2.9. Then, we have*

$$\omega_0 = 1, \quad \omega_l < 0, \quad |\omega_{l+1}| < |\omega_l|, \quad l = 1, 2, \cdots$$

$$\omega_0 = -\sum_{l=1}^{\infty} \omega_l > -\sum_{l=1}^{m} \omega_l > 0, \quad l = 1, 2, \cdots$$

$$b_{k-1} = \sum_{l=0}^{k-1} \omega_l = \frac{\Gamma(k-\beta)}{\Gamma(1-\beta)\Gamma(k)} = \frac{k^{-\beta}}{\Gamma(1-\beta)} + O\left(k^{-1-\beta}\right), \quad k = 1, 2, \cdots$$

Furthermore, with $b_0 = \omega_0 = 1$ and $(b_l - b_{l-1}) = \omega_l < 0$ for $l > 0$.

For convenience, we define the norm $|||\cdot|||_1$ as

$$|||\, U^k|||_1^2 = \| U^k\|_2^2 + \frac{\beta}{2}\tau^{\beta} \,\| (-D)^{\frac{1}{2}} U^k\|_2^2,$$

where $\{U^k\}$ are defined by (8), (18), and (19) for 1D/2D/3D respectively.

*Note that **MS1–MS3** are equivalent to (20), (22), and (22), we now show that schemes (20), (22), and (22) are unconditionally stable.*

Theorem 5.1 *The fully discrete schemes of (20), (22), and (22) are unconditionally stable in the sense that for all $h > 0$ and $\tau > 0$, there exists a positive constant C independent of τ and h, such that*

$$|||\, U^k \,|||_1 \leq 2 \,\| \, U^0 \,\|_2 + 2C \max_{0\leq k\leq M} \,\| \, F^{k-\frac{\beta}{2}} \,\|, \quad k = 1, \ldots, M.$$

Proof Writing (20) or (22) or (22) in matrix form and taking the inner product with U^m yields

$$\left(\frac{1}{\tau^{\beta}} \sum_{l=0}^{k} \omega_l \left(U^{k-l} - U^0\right), U^k\right) = \frac{\beta}{2}\left(DU^{k-1}, U^k\right) + \left(1 - \frac{\beta}{2}\right)\left(DU^k, U^k\right) + \left(F^{k-\frac{\beta}{2}}, U^k\right).$$

Using the property $b_l - b_{l-1} = \omega_l$ (see Lemma 5.1), we rewrite the above formula as

$$\begin{aligned}
&\| U^k\|_2^2 + \tau^\beta(1-\frac{\beta}{2}) \| (-D)^{\frac{1}{2}} U^k\|_2^2 \\
=\ & \tau^\beta \frac{\beta}{2} \left(DU^{k-1}, U^k\right) + \sum_{l=1}^{k} (b_{l-1}-b_l) \left(U^{k-l}, U^k\right) + b_k \left(U^0, U^k\right) \\
&+\tau^\beta \left(F^{k-\frac{\beta}{2}}, U^k\right).
\end{aligned}$$

Using $b_l - b_{l-1} < 0$, $b_k > 0$, and the Cauchy-Schwartz inequality yields

$$\begin{aligned}
&\| U^k\|_2^2 + \tau^\beta \left(1-\frac{\beta}{2}\right) \| (-D)^{\frac{1}{2}} U^k\|_2^2 \\
\le\ & \tau^\beta \frac{\beta}{4} \left(\| (-D)^{\frac{1}{2}} U^{k-1}\|_2^2 + \| (-D)^{\frac{1}{2}} U^k\|_2^2\right) + \frac{1}{2} \sum_{l=1}^{k} (b_{l-1}-b_l) \\
&\times \left(\| U^{k-l}\|_2^2 + \| U^k\|_2^2\right) b_k \| U^0\|_2^2 + \frac{b_k}{4} \| U^k\|_2^2 + \frac{\tau^{2\beta}}{bk} \| F^{k-\frac{\beta}{2}}\|_2^2 \\
&+\frac{b_k}{4} \| U^k\|_2^2. \qquad (24)
\end{aligned}$$

Note that $\left(1-\frac{\beta}{2}-\frac{\beta}{4}\right) > \frac{\beta}{4}$ and $b_0 - b_1 = \beta$, hence, we have from (24)

$$||| U^k|||_1^2 \le \sum_{l=1}^{k} (b_{l-1}-b_l) ||| U^{k-l}|||_1^2 + 2b_k \| U^0\|_2^2 + \frac{2\tau^{2\beta}}{bk} \| F^{k-\frac{\beta}{2}}\|_2^2. \qquad (25)$$

Then, by Lemma 5.1, there exist a positive constant C, such that

$$\frac{\tau^{2\beta}}{b_k} = b_k \frac{\tau^{2\beta}}{b_k^2} \le b_k \tau^{2\beta} \left(Ck^{2\beta}\right) \le CT^{2\beta}. \qquad (26)$$

Combining (25) and (26) yields

$$||| U^k|||_1^2 \le \sum_{l=1}^{k} (b_{l-1}-b_l) ||| U^{k-l}|||_1^2 + b_k \left(2 \| U^0\|_2^2 + 2C \| F^{k-\frac{\beta}{2}}\|_2^2\right). \qquad (27)$$

Denote by

$$E = 2 \| U^0\|_2^2 + 2C \max_{0\le k\le M} \| F^{k-\frac{\beta}{2}}\|_2^2.$$

Then, we have from (27)

$$||| U^k|||_1^2 \le \sum_{l=1}^{k} (b_{l-1}-b_l) ||| U^{k-l}|||_1^2 + b_k E.$$

The desired result then follows by induction. □

Theorem 5.2 *Suppose that* $u(\boldsymbol{x},t) \in C^2\left(0,T;C^5(\Omega)\right)$ *and* $\frac{\partial^m u(\boldsymbol{x},t)}{\partial \boldsymbol{x}^m}|_{\boldsymbol{x}\in\partial\Omega} = 0$ $(m = 0,1,\cdots,5)$. *If* $u(\boldsymbol{x},t)$ *is the solution of problem (1) and* $u_i^k/u_{ij}^k/u_{ijl}^k$ *are*

the difference solutions of schemes (8)/(18)/(19) at grid points (x_i, t_k)/(x_i, y_j, t_k)/(x_i, y_j, z_l, t_k) *respectively. Then, there exists positive constant* $\widetilde{C}$ *such that*

$$\| e^k \|_2 \leq \widetilde{C}(\tau^2 + h^3), \quad k = 1, 2, \ldots, M.$$

Proof We can easily get the following error equation for (20) or (22) or (22)

$$\frac{1}{\tau^\beta} \sum_{l=0}^{k} \omega_l \left(e^{k-l} - e^0 \right) = \frac{\beta}{2} D e^{k-1} + \left(1 - \frac{\beta}{2} \right) D e^k + R^k.$$

where $R^k = O\left(\tau^2 + h^3\right)$ is the truncation error at t_k.

Then, according to Theorem 5.1, the desired result can be obtained directly. □

6 Numerical experiments

In this section, three numerical examples are presented to confirm our theoretical statements. For the purpose of accuracy investigation, we compute the errors in two discrete norms: L^2 and L^∞, which denoted as L^2-err and L^∞-err, respectively. And the L^∞ errors are also plotted in a log-log graph.

Moreover, in the following examples, one can find that the conditions $\frac{\partial^k u(X,t)}{\partial X^k}|_{X=\partial\Omega} = 0$ $(k = 0, 1, \cdots, M)$ with $\Omega = [0, 1]^n (n = 1, 2, 3)$ in Theorems 3.3, 4.2 and 4.4 are not satisfied any longer. But the obtained results tell us that these conditions of the above convergence theorems might be relaxed.

6.1 Problem 1

We firstly consider the 1D time-space fractional diffusion equation. The exact analytical solution and the corresponding forcing term and initial condition are given by

$$\begin{cases} u(x,t) = (t^2+1)x^3(1-x)^3, \\ u_0(x) = x^3(1-x)^3, \\ f(x,t) = \left(\frac{2}{\Gamma(3-\beta)} t^{2-\beta} + \frac{1}{\Gamma(1-\beta)} t^{-\beta} \right) x^3(1-x)^3 \\ \qquad - \left(t^2+1\right) \left(\frac{\Gamma(4)}{\Gamma(4-\alpha)} x^{3-\alpha} - \frac{3\Gamma(5)}{\Gamma(5-\alpha)} x^{4-\alpha} + \frac{3\Gamma(6)}{\Gamma(6-\alpha)} x^{5-\alpha} - \frac{\Gamma(7)}{\Gamma(7-\alpha)} x^{6-\alpha} \right). \end{cases}$$

6.1.1 Spatial convergence text

We first investigate the spatial convergence rate. To this end, $T = 1$ and temporal stepsize $\tau = 10^{-3}$ are chosen such that the errors stemming from the temporal approximation is negligible. Since schemes **S1** and **MS1** are obtained based on the same space discrete method, we only use scheme **S1** to complete our goal. Furthermore, in order to compare the performance of our method with that of the other third-order algorithms for Rimann-Liouville fractional derivative, the methods in [24, 25] are also considered. The numerical results and the

computational times (in seconds) for $\beta = 0.5$ and different α are presented in Tables (1, 2, and 3), where the corresponding results by schemes in [24, 25] are also included.

By comparing these data, scheme **S1** seems to have the best accuracy/efficiency/stability for this problem. The scheme in [24] is unstable for small α (i.e., $\alpha = 1.2$) (see Table 1). According to Tables 1, 2, and 3, with a moderate spatial scales, there appears to be very little advantage to use the scheme in [25], which is both low accuracy and time consuming. For example, when $\alpha = 1.8$ and $h = \frac{1}{128}$ (see Table 3), the L^2 error is 5.35×10^{-8} (with CPU = 230.62) by our scheme; however, the L^2 errors by the schemes in [24] and [25] are 3.67×10^{-7} (with CPU = 199.65) and 1.07×10^{-5} (with CPU = 514.15).

Furthermore, we find that the scheme **S1** yields a higher spacial approximation order than theoretical value 3 for $\alpha = 1.5$ and $\alpha = 1.8$. For example, when $\alpha = 1.8$, the experimentally determined order is almost 3.7. In order to further study the relationship between α and the spatial convergence rate, we plot L^{∞}_{Rate} as a function of α and β at $T = 1$ with $h = 1/50$ and $\tau = 1/1000$, as shown in Fig. 1. From which, we find that the spatial approximation order is close to $2 + \alpha$, which agrees with the conjecture in Remark 3.2.

Remark 6.1 In fact, we also tested Problem 1 with different α. However, numerical experiments illustrate that the algorithm in [24] is unstable for $\alpha \in (1, 1.35]$. Due to the complexity of the coefficient matrix (denoted by A) for the resulted third-order scheme from [24], it is hard to obtain the spectral radius of A by theory analysis.

Table 1 Numerical results and CPU times (in seconds) of several difference schemes for Problem 1 with $\alpha = 1.2$, $\beta = 0.5$, $T = 1$, and $\tau = 10^{-3}$

	h	$\frac{1}{16}$	$\frac{1}{32}$	$\frac{1}{64}$	$\frac{1}{128}$
Our scheme **SI**	L^2-err	2.25e−4	3.48e−5	4.30e−6	4.62e−7
	Rate	–	2.69	3.02	3.22
	L^{∞}-err	3.61e−4	6.19e−5	8.63e−6	1.06e−6
	Rate	–	2.55	2.84	3.03
	CPU	6.22	12.17	23.59	210.85
Scheme in [24]	L^2-err	7.68e+4	5.39e+46	NaN	NaN
	Rate	–	–	–	–
	L^{∞}-err	2.27e+5	1.61e+47	NaN	NaN
	Rate	–	–	–	–
	CPU	5.99	11.08	22.31	228.42
Scheme in [25]	$ER_{L^{\infty}}$	1.69e+4	3.38e−5	4.59e−6	6.08e−7
	Rate	–	–	2.88	2.92
	ER_{L^2}	6.76e+4	5.63e−5	9.54e−6	1.61e−6
	Rate	–	–	2.56	2.57
	CPU	9.78	26.18	106.64	509.12

Table 2 Numerical results and CPU times (in seconds) of several difference schemes for Problem 1 with $\alpha = 1.5$, $\beta = 0.5$, $T = 1$, and $\tau = 10^{-3}$

	h	$\frac{1}{16}$	$\frac{1}{32}$	$\frac{1}{64}$	$\frac{1}{128}$
Our scheme **SI**	L^2-err	1.74e−4	1.94e−5	1.75e−6	1.34e−7
	Rate	–	3.16	3.48	3.71
	L^∞-err	2.95e−4	3.75e−5	4.10e−6	4.09e−7
	Rate	–	2.98	3.19	3.33
	CPU	6.04	11.78	23.67	214.81
Scheme in [24]	L^2-err	1.89e−4	2.59e−56	3.42e−6	4.29e−7
	Rate	–	2.87	2.92	2.99
	L^∞-err	3.48e−4	4.88e−5	6.33e−6	7.92e−7
	Rate	–	2.84	2.95	3.00
	CPU	5.79	10.89	21.90	199.65
Scheme in [25]	ER_{L^∞}	3.38e−4	5.48e−5	9.02e−6	1.52e−6
	Rate	–	2.62	2.60	2.57
	ER_{L^2}	6.48e−4	1.13e−4	2.30e−5	3.96e−6
	Rate	–	2.52	2.30	2.53
	CPU	11.67	29.83	126.44	571.10

Thus, let us analyze $\rho(A)$ numerically. Figure 2 shows the varying of $\rho(A)$ with α. We can see that $\rho(A) > 1$ when $\alpha \in (1, 1.35]$; thus, the resulted scheme in [24] is unstable at this case.

Table 3 Numerical results and CPU times (in seconds) of several difference schemes for Problem 1 with $\alpha = 1.8$, $\beta = 0.5$, $T = 1$, and $\tau = 10^{-3}$

	h	$\frac{1}{16}$	$\frac{1}{32}$	$\frac{1}{64}$	$\frac{1}{128}$
Our scheme **SI**	L^2-err	1.09e−4	9.47e−6	6.93e−7	5.35e−8
	Rate	–	3.52	3.77	3.70
	L^∞-err	1.90e−4	1.82e−5	1.50e−6	1.17e−7
	Rate	–	3.38	3.60	3.69
	CPU	6.18	11.92	27.08	230.62
Scheme in [24]	L^2-err	1.50e−4	2.16e−56	2.89e−6	3.67e−7
	Rate	–	2.79	2.90	2.98
	L^∞-err	2.55e−4	3.72e−5	4.97e−6	6.32e−7
	Rate	–	2.78	2.90	2.98
	CPU	5.63	10.95	21.83	197.58
Scheme in [25]	L^2-err	9.73e−4	2.20e−4	4.88e−5	1.07e−5
	Rate	–	2.14	2.17	2.19
	L^∞-err	1.62e−3	4.44e−4	9.91e−5	2.10e−5
	Rate	–	1.87	2.16	2.24
	CPU	9.77	26.97	113.96	514.15

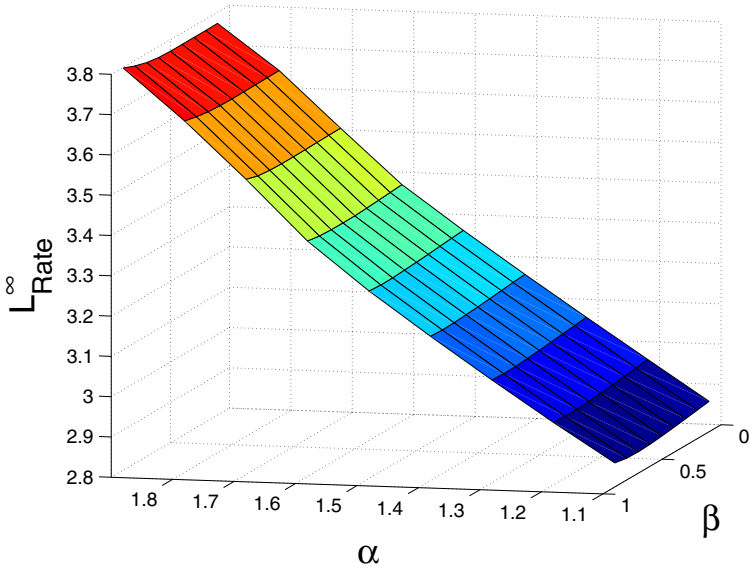

Fig. 1 The spatial convergence rate as a function of α and β for Problem 1

6.1.2 Temporal convergence text

Now, we check the temporal accuracy of the schemes **S1** and **MS1**. By fixed, the space step is sufficiently small to avoid contamination of the spatial error. In Tables 4 and 5, the numerical results at $T = 5$ corresponding to **S1** and **MS1** are presented with $h = 1/500$ and different τ. Clearly, Table 2 shows that scheme **SI** yields

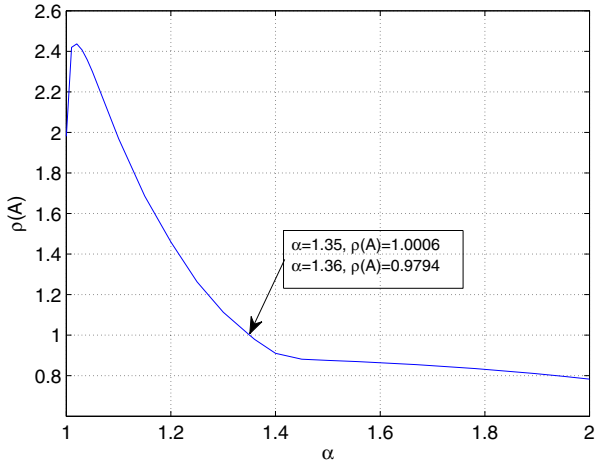

Fig. 2 The spectral radius of the coefficient matrix for the resulted third-order scheme from [24]

Table 4 Numerical results using scheme **S1** for Problem 1 at $T = 5$ with $h = 1/500$

	$\alpha = 1.2$			$\alpha = 1.5$		$\alpha = 1.8$	
τ	β	L^2-err	L^∞-err	L^2-err	L^∞-err	L^2-err	L^∞-err
5/10	0.2	1.33e−4	1.97e−4	8.60e−5	1.25e−4	5.56e−5	8.07e−5
5/20		4.07e−5	6.02e−5	2.64e−5	3.84e−5	1.71e−5	2.48e−5
5/40		1.20e-5	1.77e-5	7.97e-6	1.15e-5	5.19e-6	7.50e-6
5/80		3.30e−6	4.79e−6	2.36e−6	3.32e−6	1.56e−6	2.25e−6
5/160		9.67e−7	1.37e−6	6.82e−7	9.06e−7	4.73e−7	6.89e−7
5/10	0.5	4.62e−4	6.85e−4	2.91e−4	4.24e−4	1.84e−4	2.67e−4
5/20		1.67e−4	2.47e−4	1.05e−4	1.53e−4	6.65e−5	9.63e−5
5/40		5.96e−5	8.83e−5	3.78e−5	5.50e−5	2.39e−5	3.45e−5
5/80		2.09e−5	3.10e−5	1.35e−5	1.96e−5	8.52e−6	1.23e−5
5/160		7.14e−6	1.05e−5	4.80e−6	6.98e−6	3.03e−6	4.37e−6
5/10	0.8	1.04e−3	1.54e−3	6.44e−4	9.36e−4	4.02e−4	5.81e−4
5/20		4.54e−4	6.73e−4	2.82e−4	4.09e−4	1.76e−4	2.54e−4
5/40		1.98e−4	2.93e−4	1.23e−4	1.78e−4	7.57e−5	1.11e−4
5/80		8.58e−5	1.27e−4	5.35e−5	7.76e−5	3.34e−5	4.83e−5
5/160		3.71e−5	5.50e−5	2.33e−5	3.37e−5	1.45e−5	2.10e−5

Table 5 Numerical results using scheme **MS1** for Problem 1 at $T = 5$ with $h = 1/500$

	$\alpha = 1.2$			$\alpha = 1.5$		$\alpha = 1.8$	
τ	β	L^2-err	L^∞-err	L^2-err	L^∞-err	L^2-err	L^∞-err
5/10	0.2	1.70e−4	2.99e−4	1.77e−4	3.09e−4	1.86e−4	3.22e−4
5/20		3.99e−5	7.05e−5	4.17e−5	7.36e−5	4.47e−5	7.79e−5
5/40		9.09e−6	1.57e−5	9.16e−6	1.64e−5	1.03e−5	1.81e−5
5/80		2.32e−6	3.49e−6	1.72e−6	3.10e−6	2.10e−6	3.80e−6
5/160		5.39e−7	8.02e−7	3.60e−7	7.47e−7	3.04e−7	5.79e−7
5/10	0.5	3.90e−4	6.78e−4	3.99e−4	6.90e−4	4.09e−4	7.03e−4
5/20		9.37e−5	1.64e−4	9.66e−5	1.68e−4	1.00e−4	1.73e−4
5/40		2.17e−5	3.83e−5	2.24e−5	3.94e−5	2.39e−5	4.15e−5
5/80		5.00e−6	8.34e−6	4.70e−6	8.46e−6	5.38e−6	9.47e−6
5/160		1.15e−6	1.82e−6	7.99e−7	1.33e−6	1.01e−6	1.86e−6
5/10	0.8	5.35e−4	9.18e−4	5.38e−4	9.22e−4	5.42e−4	9.29e−4
5/20		1.32e−4	2.28e−4	1.33e−4	2.29e−4	1.35e−4	2.31e−4
5/40		3.25e−5	5.61e−5	3.26e−5	5.62e−5	3.32e−5	5.70e−5
5/80		7.97e−6	1.38e−5	7.76e−6	1.35e−5	8.05e−6	1.39e−5
5/160		2.13e−6	3.48e−6	1.71e−6	3.02e−6	1.86e−6	3.24e−6

a temporal approximation order close to $2-\beta$, which is fit with the theoretical estimations. Again, all the results are plotted in a log-log graph (see Fig. 3a, c, e) and the slopes of the error curves in these log-log plots are 1.8, 1.5, and 1.2 respectively

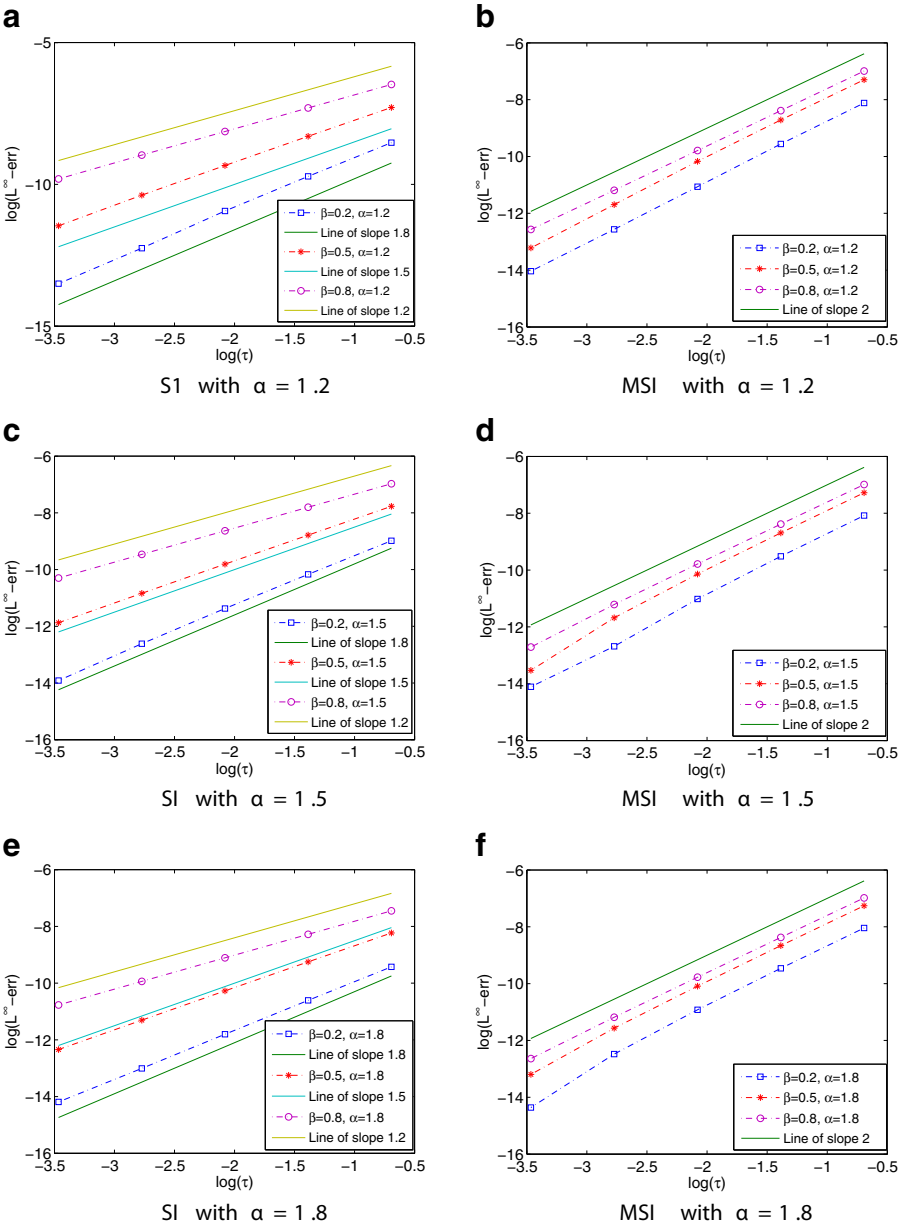

Fig. 3 L^{∞}-err as a function of the time step τ for Problem 1. **a**, **c**, **e** Corresponding to Table 2. **b**, **d**, **f** Corresponding to Table 3

for $\beta = 0.2, 0.5, 0.8$. Compared with the scheme **S1**, the data in Table 3 indicate that scheme **MS1** is second-order accurate in time, which can be observed more intuitive from Fig. 3b, d, f.

Moreover, we plot the temporal convergence rate L^{∞}_{Rate} as a function of α and β at $T = 5$ with $h = 1/256$ and $\tau = 5/80$, as shown in Fig. 4, which further confirms temporal approximation orders of schemes **S1** and **MS1** close to 2-β and 2, respectively.

6.2 Problem 2

In order to further study the order of convergence in space of scheme **S1** and compare the accuracy and stability of the proposed method with the schemes in [24, 25], we calculated a second 1D test problem with a smooth solution. The exact analytical solution and the corresponding forcing term and initial condition are given by

$$\begin{cases} u(x,t) = \left(t^{3+\beta}+1\right)\sin^3(\pi x), \\ u_0(x) = \sin^3(\pi x), \\ f(x,t) = \left(\frac{2}{\Gamma(3-\beta)}t^{2-\beta} + \frac{1}{\Gamma(1-\beta)}t^{-\beta}\right)\sin(\pi x)^3 \\ \qquad -(t^{3+\beta}+1)\frac{1}{\Gamma(3-\alpha)}\int_0^x (x-\xi)^{2-\alpha}\left[27\pi^3\cos^3(\pi\xi) - 21\pi^3\cos(\pi\xi)\right]d\xi. \end{cases}$$

For convenience, we only investigate the spatial convergence rate with $\beta = 0.5$ and $\alpha = 1.3$, $\alpha = 1.7$. Choosing $T = 1$ and $\tau = 2.5 \times 10^{-4}$, the numerical results and the computational times (in seconds) for our scheme **S1** and schemes in [24, 25] are presented in Tables 6 and 7. Again, by comparing these data, scheme **S1** seems to have the best accuracy/efficiency/stability for this problem.

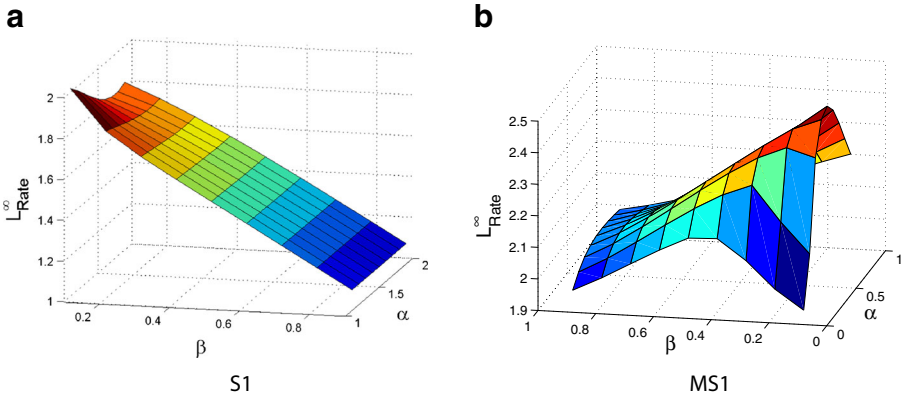

Fig. 4 The temporal convergence rate as a function of α and β for solving Problem 1 using schemes **a S1**. **b MS1**

Table 6 Numerical results and CPU times (in seconds) of several difference schemes for Problem 2 with $\alpha = 1.3$, $\beta = 0.5$, $T = 1$, and $\tau = 2.5 \times 10^{-4}$

	h	$\frac{1}{16}$	$\frac{1}{32}$	$\frac{1}{64}$	$\frac{1}{128}$
Our scheme **SI**	L^2-err	1.04e−2	1.07e−3	1.09e−4	1.11e−5
	Rate	–	3.27	3.30	3.29
	L^∞-err	1.74e−2	2.04e−3	2.15e−4	2,22e−5
	Rate	–	3.10	3.24	3.28
	CPU	4.17	9.69	28.50	138.20
Scheme in [24]	L^2-err	2.05e−1	1.01e3	1.37e23	Inf
	Rate	–	–	–	–
	L^∞-err	4.79e−1	2.99e3	6.55e23	Inf
	Rate	–	–	–	–
	CPU	4.88	10.56	28.92	167.30
Scheme in [25]	ER_{L^∞}	NaN	2.39e0	4.01e−4	5.87e−4
	Rate	–	–	–	–
	ER_{L^2}	NaN	1.31e1	9.79e−4	4.49e−3
	Rate	–	–	–	–
	CPU	9.30	30.39	145.27	689.48

Remark 6.2 Moreover, comparing the numerical results of Problems 1 and 2, we find that the spatial convergence rate may also have a certain relationship with the smoothness of the exact solution. We hope to investigate this important issue in the future.

Table 7 Numerical results and CPU times (in seconds) of several difference schemes for Problem 2 with $\alpha = 1.7$, $\beta = 0.5$, $T = 1$, and $\tau = 2.5 \times 10^{-4}$

	h	$\frac{1}{16}$	$\frac{1}{32}$	$\frac{1}{64}$	$\frac{1}{128}$
Our scheme SI	L^2-err	4.70e−3	3.52e−4	3.82e−5	5.05e−6
	Rate	–	3.74	3.20	2.92
	L^∞-err	8.35e−3	6.16e−4	6.20e−5	7.45e−6
	Rate	–	3.76	3.31	3.05
	CPU	3.60	8.10	25.24	124.44
Scheme in [24]	L^2-err	9.11e−3	1.17e−3	1.46e−4	1.81e−5
	Rate	–	2.96	2.99	3.01
	L^∞-err	1.65e−2	2.17e−3	2.74e−4	3.38e−5
	Rate	–	2.93	2.99	3.02
	CPU	4.85	10.25	28.60	145.52
Scheme in [25]	ER_{L^∞}	2.86e−2	5.18e−3	9.56e−4	1.85e−4
	Rate	–	2.47	2.44	2.37
	ER_{L^2}	5.63e−2	1.10e−2	2.08e−3	3.87e−4
	Rate	–	2.36	2.40	2.43
	CPU	9.28	30.06	144.35	715.34

6.3 Problem 3

Now, we consider the 2D time-space fractional diffusion equation. The exact analytical solution and the corresponding forcing term and initial condition are given by

$$\begin{cases} u(x,y,t)=(t^3+1)x^3(1-x)^3y^3(1-y)^3, \\ u_0(x,y)=x^3(1-x)^3y^3(1-y)^3, \\ f(x,y,t)=\left(\frac{6}{\Gamma(4-\beta)t^{3-\beta}}+\frac{1}{\Gamma(1-\beta)}t^{-\beta}\right)x^3(1-x)^3y^3(1-y)^3 \\ \qquad -(t^3+1)y^3(1-y)^3\left(\frac{\Gamma(4)}{\Gamma(4-\alpha_1)}x^{3-\alpha_1}-\frac{3\Gamma(5)}{\Gamma(5-\alpha_1)}x^{4-\alpha_1}+\frac{3\Gamma(6)}{\Gamma(6-\alpha_1)}x^{5-\alpha_1}-\frac{\Gamma(7)}{\Gamma(7-\alpha_1)}x^{6-\alpha_1}\right) \\ \qquad -(t^3+1)x^3(1-x)^3\left(\frac{\Gamma(4)}{\Gamma(4-\alpha_2)}y^{3-\alpha_2}-\frac{3\Gamma(5)}{\Gamma(5-\alpha_1)}y^{4-\alpha_1}+\frac{3\Gamma(6)}{\Gamma(6-\alpha_2)}y^{5-\alpha_1}-\frac{\Gamma(7)}{\Gamma(7-\alpha_2)}y^{6-\alpha_2}\right). \end{cases}$$

Without loss of generality, we only choose $\beta = 0.5$ to verify the numerical accuracy and efficiency of schemes **S2** and **MS2**.

6.3.1 Spatial convergence text

Firstly, the numerical accuracy in space is verified. Once again, we only use scheme **S2** to complete our goal due to the space discrete methods of both schemes **S2** and **MS2** are same. Choosing $T = 0.1$, then taking a fixed temporal stepsize $\tau = 10^{-4}$ and varying spatial stepsize h, we obtain computational results for $\beta = 0.5$ displayed in Table 8, from which we see that the spacial approximation order is higher than theoretical value 3.

Once again, in order to further verify the spatial accuracy, we plot the spatial convergence rate L^{∞}_{Rate} as a function of α_1 and α_2 at $T = 0.1$ with $\tau = 10^{-4}$, $h = 1/50$ and $\beta = 0.5$, as shown in Fig. 5, which shows that the spatial approximation order depends on α_1 and α_2.

Table 8 Numerical results using scheme **S2** for Problem 3 at $T = 0.1$ with $\tau = 10^{-4}$ and $\beta = 0.5$

	h	$\frac{1}{16}$	$\frac{1}{32}$	$\frac{1}{64}$	$\frac{1}{128}$
$\alpha_1 = \alpha_2$=1.2	L^2-err	9.35e−7	1.69e−7	2.38e−8	3.12e−9
	Rate	–	2.47	2.83	2.93
	L^∞-err	2.59e−6	5.00e−7	7.86e−8	1.06e−8
	Rate	–	2.37	2.66	2.89
$\alpha_1 = \alpha_2$=1.5	L^2-err	7.28e−7	8.88e−8	9.04e−9	1.06e−9
	Rate	–	3.04	3.30	3.09
	L^∞-err	1.96e−6	2.72e−7	3.01e−8	2.94e−9
	Rate	–	2.98	3.19	3.32
$\alpha_1 = \alpha_2$=1.8	ER_{L^∞}	3.00e−7	3.01e−8	2.53e−9	2.23e−10
	Rate	–	3.32	3.57	3.50
	ER_{L^2}	1.05e−6	1.22e−7	1.10e−8	8.91e−10
	Rate	–	3.11	3.46	3.63

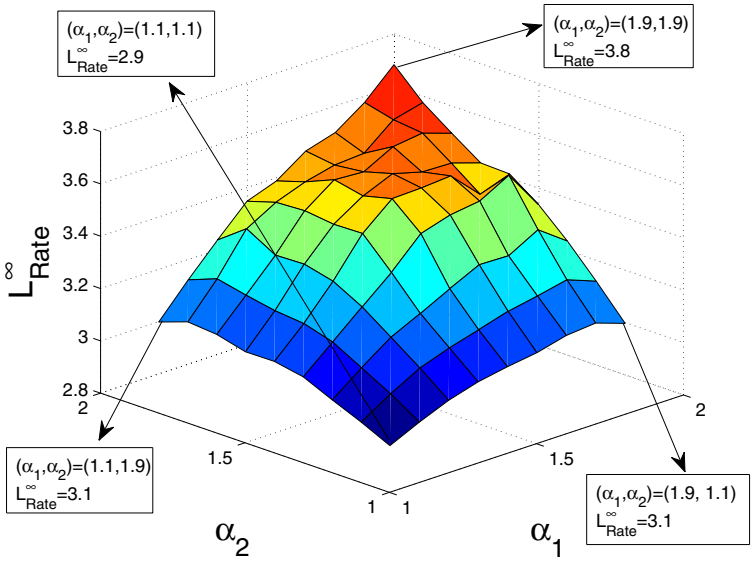

Fig. 5 The spatial convergence rate as a function of α_1 and α_2 with $h = 1/50$ for Problem 3

6.3.2 Temporal convergence text

To verify the temporal accuracy of the schemes **S2** and **MS2**, with a fixed and sufficiently small spatial stepsize $h = 1/100$, and different temporal stepsize τ, the numerical results for $T = 5$ using both schemes are listed in Tables 9 and 10, respectively. From the data of these tables, we can say that the computational errors of the scheme **MS2** are smaller than those of **S2**. However, Fig. 6a, b illustrates that the accuracy of both schemes in temporal direction is 2.5-order. Thus, we guess that the splitting error totally dominates the error for the AD procedure, i.e., the perturbation errors (13) and (23) are much larger than the time

Table 9 Numerical results using scheme **S2** for Problem 3 at $T = 5$ with $h = 1/100$ and $\beta = 0.5$

	$(\alpha_1, \alpha_2) = (1.2, 1.7)$		$(\alpha_1, \alpha_2) = (1.5, 1.5)$		$(\alpha_1, \alpha_2) = (1.8, 1.6)$	
τ	L^2-err	L^∞-err	L^2-err	L^∞-err	L^2-err	L^∞-err
5/10	1.17e−3	3.36e−3	1.17e−3	3.68e−3	1.39e−3	4.80e−3
5/20	2.04e−4	5.85e−4	2.08e−4	6.62e−4	2.60e−4	8.90e−4
5/40	3.62e−5	1.03e−4	3.72e−5	1.19e−4	4.67e−5	1.59e−4
5/60	1.31e−5	3.72e−5	1.35e−5	4.24e−5	1.69e−5	5.79e−5
5/80	6.33e−6	1.81e−5	6.53e−6	2.07e−5	8.19e−6	2.80e−5
5/100	3.68e−6	1.05e−5	3.72e−6	1.19e−5	4.66e−6	1.59e−5

Table 10 Numerical results using scheme **MS2** for Problem 3 at $T = 5$ with $h = 1/100$ and $\beta = 0.5$

	$(\alpha_1, \alpha_2) = (1.2, 1.7)$		$(\alpha_1, \alpha_2) = (1.5, 1.5)$		$(\alpha_1, \alpha_2) = (1.8, 1.6)$	
τ	L^2-err	L^∞-err	L^2-err	L^∞-err	L^2-err	L^∞-err
5/10	7.67e−4	2.27e−3	8.36e−4	2.57e−3	9.97e−4	3.36e−3
5/20	1.40e−4	4.27e−4	1.50e−4	4.79e−4	1.81e−4	6.13e−4
5/40	2.64e−5	8.10e−5	2.77e−5	8.84e−5	3.39e−5	1.15e−4
5/60	8.99e−6	2.54e−5	1.04e−6	3.31e−5	1.26e−5	4.27e−5
5/80	4.13e−6	1.16e−5	5.22e−6	1.69e−5	6.29e−6	2.12e−5
5/100	2.32e−6	6.32e−6	3.17e−6	1.02e−5	3.67e−6	1.24e−5

truncation errors of schemes **S2** and **MS2**. To further verify our speculation, we plot

$$\mathrm{Div}(\tau, \alpha_1, \alpha_2) = \frac{L^\infty\text{-err}(\tau, \alpha_1, \alpha_2, \mathrm{MS2})}{L^\infty\text{-err}(\tau, \alpha_1, \alpha_2, \mathrm{S2})}$$

as a function of τ, as shown in Fig. 7, where L^∞-err$(\tau, \alpha_1, \alpha_2, \mathrm{S2})$ and L^∞-err$(\tau, \alpha_1, \alpha_2, \mathrm{MS2})$ denote the L^∞ errors which correspond to the results from Tables 9 and 10 respectively. It is observed that there are a large group of numerical results around a value near $\left(\frac{1-\frac{\beta}{2}}{\Gamma(2-\beta)}\right)^2 = 0.7162$, which is in good agreement with the proportion of perturbation errors (23) and (13). Of course, the dominant role of the splitting error will gradually diminished as the time step approaches zero. The same phenomenon has been observed in [36].

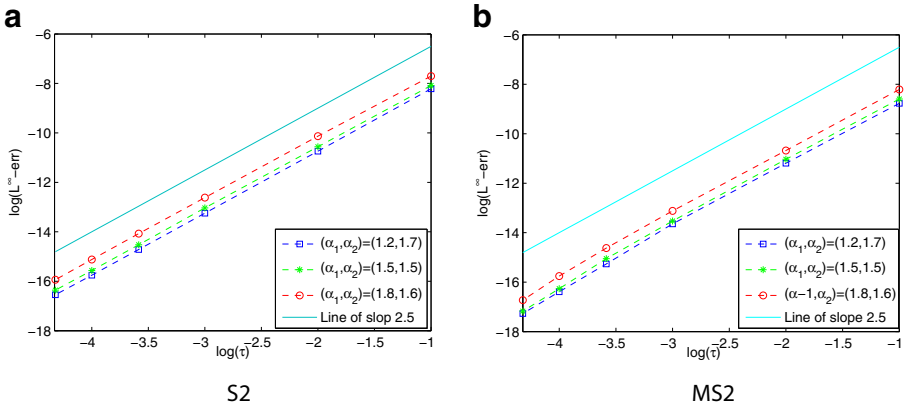

Fig. 6 L^∞-err as a function of the time step τ for Problem 3 corresponding to **a** Table 5 and **b** Table 6

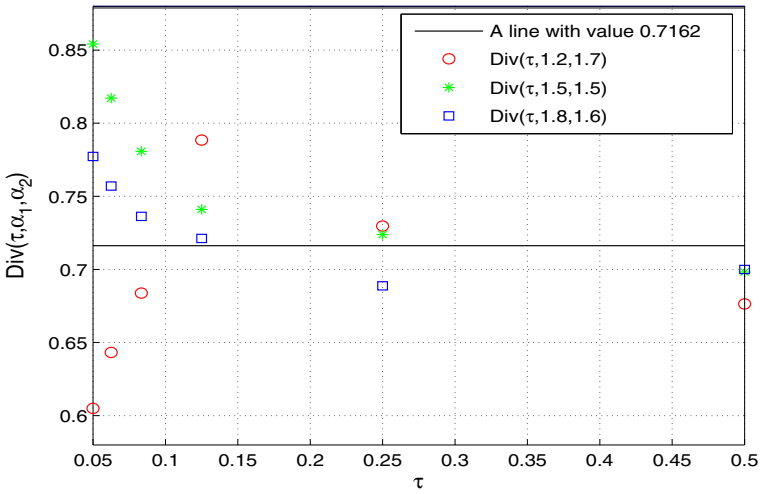

Fig. 7 $\mathrm{Div}(\tau, \alpha_1, \alpha_2) = \frac{L^\infty\text{-err}(\tau,\alpha_1,\alpha_2,\mathrm{MS2})}{L^\infty\text{-err}(\tau,\alpha_1,\alpha_2,\mathrm{S2})}$ as a function of τ

6.4 Problem 4

By the last example we attempt to verify the accuracy of schemes **S3** and **MS3** for 3D case. The exact solution and the initial value on $(0, 1)^3 \times (0, T]$ are given by

$$\begin{cases} u(x, y, z, t) = (t^3 + 1)x^3(1 - x)^3y^3(1 - y)^3z^3(1 - z)^3, \\ u_0(x, y, z) = x^3(1 - x)^3y^3(1 - y)^3z^3(1 - z)^3. \end{cases}$$

The function f can easily be obtained with the help of the source term in Problem 2. Without loss of generality, we only choose β=0.5 and α_1=α_2=α_3=1.5 to verify the numerical accuracy and efficiency of schemes **S3** and **MS3**.

Firstly, the numerical accuracy in space is verified. Once again, we only use scheme **S3** to complete our goal. Choosing T=10^{-3}, then taking a fixed temporal stepsize τ=10^{-5} and varying spatial stepsize h, we obtain the computational results shown in Table 11 which confirmed that the convergence order of the scheme **S3** in space is three.

Secondly, we check the temporal accuracy of the schemes **S3** and **MS3**. With the fixed spatial stepsize h=$\frac{1}{50}$, the computational results at T=1 are reported in Table 12, from which we can see that both schemes produced very similar results and the convergence orders are round 2.5, which are much better than the theoretical estimates.

Table 11 Numerical results using schemes **S3** for Problem 4 at $T = 10^{-3}$ with $\tau = 10^{-5}$, $\beta = 0.5$, $\alpha_1 = \alpha_2 = \alpha_3 = 1.5$, and different h

h	$\frac{1}{12}$	$\frac{1}{24}$	$\frac{1}{36}$	$\frac{1}{48}$
L^2-err	7.70e−9	1.32e−9	3.93e−10	1.60e−10
Rate	-	2.55	2.98	3.13
L^∞-err	3.59e−8	7.72e−9	2.48e−9	1.04e−9
Rate	-	2.22	2.80	3.01

Table 12 Numerical results using schemes **S3** and **MS3** for Problem 4 at $T = 1$ with $h = 1/50$, $\beta = 0.5$, $\alpha_1 = \alpha_2 = \alpha_3 = 1.5$, and different τ

	τ	$\frac{1}{5}$	$\frac{1}{10}$	$\frac{1}{20}$	$\frac{1}{40}$
S3	L^2-err	3.69e−7	1.22e−7	1.93e−8	3.15e−9
	Rate	–	1.60	2.66	2.61
	L^∞-err	2.13e−6	7.26e−7	1.17e−7	1.87e−8
	Rate	–	1.56	2.63	2.64
MS3	L^2-err	3.21e−7	8.37e−8	1.30e−8	2.22e−9
	Rate	–	1.94	2.69	2.54
	L^∞-err	1.83e−6	4.79e−7	7.62e−8	1.32e−8
	Rate	–	1.94	2.65	2.53

This further illustrate that the splitting error totally dominates the error for the AD procedure.

7 Conclusions

In this paper, based on the Caputo fractional derivative in time and the Riemann-Liouville fractional derivatives in space, two kinds of high-precision unconditionally stable finite difference methods have been proposed and studied for the 1D/2D/3D time-space fractional diffusion equations. The theoretical analysis of the stability and convergence is presented in details. Numerical experiments illustrated the availability of the both methods and the high accuracy of these difference schemes. Moreover, numerical results also illustrate that the spacial approximation order is higher than theoretical value 3 in some cases, and Remark 3.2 provided a reasonable explanation.

Moreover, we can further improve the accuracy by the Richardson extrapolation technique [20] or constructing compact operators [20, 35]. The research on these aspects will be reported in our future work.

Acknowledgements Authors thank the editor and referees for their constructive comments and useful suggestions which improved greatly the quality of our paper.

Funding information The work was partially supported by the CAPES and CNPq, Brazil; the NSF of China (Nos. 1701196, 11701197); the China Postdoctoral Sustentation Fund; the Natural Science Foundation of Fujian Province (No. 2016J05007); the Natural Science Foundation of Xinjiang Province (No. 2016D01C07) and the Promotion Program for Young and Middle-aged Teacher in Science and Technology Research of Huaqiao University (ZQN-YX502), China.

Appendix

In this appendix, we present the proof of $h(\alpha; x) \leq 0$. Thus, we list the following lemma.

Lemma A.1 *For any $x \in [0, \pi]$ and $\alpha \in (1, 2)$, we have $h(\alpha; x)$ decreases with respect to α, that is*

$$\frac{\partial}{\partial \alpha} h(\alpha; x) \leq 0.$$

Proof Taking the partial derivative of $h(\alpha, x)$ with respect to α, we have

$$\frac{\partial}{\partial \alpha} h(\alpha; x) = L_1(\alpha; x) + \frac{\pi - x}{2} L_2(\alpha; x), \tag{28}$$

where

$$L_1(\alpha, x) = \frac{6\alpha - 7}{24} \cos(A-x) + \frac{-6\alpha + 13}{12} \cos(A) + \frac{6\alpha - 19}{24} \cos(A+x),$$

$$L_2(\alpha, x) = \frac{3\alpha^2 - 7\alpha}{24} \sin(A-x) + \frac{-3\alpha^2 + 13\alpha}{12} \sin(A) + \frac{3\alpha^2 - 19\alpha + 24}{24} \sin(A+x)$$

with $A = \frac{\alpha(x-\pi)}{2} - x$.

Next, we estimate Eq. 28 via the following two steps.

I: We first consider $L_1(\alpha; x) \leq 0$. It is easy to obtain

$$L_1(\alpha, x) = \frac{6\alpha - 13}{12} \cos(A) \cos(x) + \frac{1}{2} \sin(A) \sin(x) + \frac{-6\alpha + 13}{12} \cos(A). \tag{29}$$

For any $x \in [\pi/2, \pi]$ and $\alpha \in (1, 2)$, it is obviously $L_1(\alpha; x) \leq 0$.

For any $x \in [0, \pi/2)$ and $\alpha \in (1, 2)$, since

$$\frac{\partial}{\partial x} \left[\frac{6\alpha - 13}{12} \cos A \cos x + \frac{1}{2} \sin A \sin x \right] \leq 0,$$

we have

$$\frac{6\alpha - 13}{12} \cos A \cos x + \frac{1}{2} \sin A \sin x \leq \frac{6\alpha - 13}{12} \cos\left(-\frac{\alpha\pi}{2}\right),$$

and combining with

$$\frac{-6\alpha + 13}{12} \cos A \leq \frac{-6\alpha + 13}{12} \cos\left(\frac{-\alpha\pi}{2}\right),$$

so we obtain $L_1(\alpha; x) \leq 0$.

II: We now consider $L_2(\alpha; x) \leq 0$. It is easy to obtain

$$L_2(\alpha; x) = \frac{3\alpha^2 - 7\alpha}{12} \sin A \cos x + \frac{2 - \alpha}{2} \sin\left(\frac{\alpha(x - \pi)}{2}\right) + \frac{-3\alpha^2 + 13\alpha}{12} \sin(A). \tag{30}$$

For any $x \in [\pi/2, \pi]$ and $\alpha \in (1, 2)$, it is obviously $L_2(\alpha; x) \leq 0$.

For any $x \in [0, \pi/2)$ and $\alpha \in (1, 2)$, we have

$$\begin{aligned} L_2(\alpha; x) &= \frac{3\alpha^2 - 7\alpha}{12} \sin A \cos x + \frac{2-\alpha}{2} \sin(A + x) + \frac{-3\alpha^2 + 13\alpha}{12} \sin(A) \\ &= \frac{3\alpha^2 - 13\alpha}{12} \sin A(\cos x - 1) + \sin A \cos x + \frac{2-\alpha}{2} \cos A \cos x \\ &\leq 0. \end{aligned}$$

As a result of (I) and (II), we obtain the expected result. □

References

1. Deng, W.H., Li, C.P.: The evolution of chaotic dynamics for fractional unified system. Phys. Lett. A **372**, 401–407 (2008)
2. Scalas, E., Gorenflo, R., Mainardi, F.: Fractional calculus and continuous time finance. Physica A **284**, 376–384 (2000)
3. Benson, D.A., Wheatcraft, S.W., Meerschaert, M.M.: Application of a fractional advection-dispersion equation. Water Resources Res. **36**, 1403-1412 (2000)
4. Sun, H.G., Zhang, Y., Baleanu, D., Chen, W., Chen, Y.Q.: A new collection of real world applications of fractional calculus in science and engineering. Commun. Nonlinear Sci. Numer. Simulat. **64**, 213-231 (2018)
5. Gorenflo, R., Mainardi, F., Moretti, D., Pagnini, G., Paradisi, P.: Fractional diffusion: probability distributions and random walk models. Physica A **305**, 106-112 (2002)
6. Chen, W.: TimeCspace fabric underlying anomalous diffusion. Chaos, Soliton. Fract. **28**, 923-929 (2006)
7. Podlubny, I.: Fractional Differential Equations. Academic Press, New York (1999)
8. Magin, R.L., Abdullah, O., Baleanu, D., Zhou, X.J.: Anomalous diffusion expressed through fractional order differential operators in the Bloch-Torrey equation. J. of Mag. Res. **190**, 255-270 (2008)
9. Liu, F., Zhuang, P., Anh, V., Turner, I.: A fractional-order implicit difference approximation for the space-time fractional diffusion equation. ANZIAM J. **47**, C48-C68 (2006)
10. Yang, Q., Turner, I., Liu, F., Ili'c, M.: Novel numerical methods for solving the time-space fractional diffusion equation in two dimensions. SIAM J. Sci. Comput. **33**, 1159-1180 (2011)
11. Wang, Z., Vong, S.K., Lei, S.L.: Finite difference schemes for two-dimensional time-space fractional differential equations. Int. J. Comput. Math. **93**, 578-595 (2016)
12. Chen, M.H., Deng, W.H.: A second-order accurate numerical method for the space-time tempered fractional diffusion-wave equation. Appl. Math. Lett. **68**, 87-93 (2017)
13. Pang, H., Sun, H.: Fourth order finite difference schemes for time-space fractional sub-diffusion equations. Comput. Math. Appl. **71**, 1287-1302 (2016)
14. Langlands, T.A.M., Henry, B.I.: The accuracy and stability of an implicit solution method for the fractional diffusion equation. J. Comput. Phys. **205**, 719-736 (2005)
15. Cui, M.R.: Compact alternating direction implicit method for two-dimensional time fractional diffusion equation. J. Comput. Phys. **231**, 2621–2633 (2012)
16. Ren, J.C., Sun, Z.Z., Zhao, X.: Compact difference scheme for the fractional sub-diffusion equation with Neumann boundary conditions. J. Comput. Phys. **232**, 456–467 (2013)
17. Zhai, S.Y., Weng, Z.F., Gui, D.W., Feng, X.L.: High-order compact operator splitting method for three-dimensional fractional equation with subdiffusion. Int. J. Heat Mass Transfer **84**, 440–447 (2015)
18. Zhai, S.Y., Feng, X.L.: A block-centered finite-difference method for the time-fractional diffusion equation on nonuniform grids. Numer. Heat Transfer **B 69**, 217-233 (2016)
19. Hao, Z.P., Sun, Z.Z., Cao, W.R.: A fourth-order approximation of fractional derivatives with its applications. J. Comput. Phys. **281**, 787-805 (2015)

20. Vong, S., Lyu, P., Chen, X., Lei, S.-L.: High order finite difference method for time-space fractional differential equations with Caputo and Riemann-Liouville derivatives. Numer Algorithms **72**, 195–210 (2016)
21. Alikhanov, A.A.: A new difference scheme for the time fractional diffusion equation. J. Comput. Phys. **280**, 424–438 (2015)
22. Tian, W.Y., Zhou, H., Deng, W.H.: A class of second order difference approximations for solving space fractional diffusion equations. Math. Comp. **84**, 1703–1727 (2015)
23. Zhou, H., Tian, W.Y., Deng, W.H.: Quasi-compact finite difference schemes for space fractional diffusion equations. J. Sci. Comput. **56**, 45–66 (2013)
24. Ding, H.F., Li, C.P.: High-order numerical algorithms for Riesz derivatives via constructing new generating functions. J. Sci. Comput. **71**, 759–784 (2017)
25. Ding, H.F., Li, C.P.: High-order algorithms for Riesz derivative and their applications (III). Fract. Calc. Appl. Anal. **19**, 19–55 (2016)
26. Wang, Z.B., Vong, S.W.: Compact difference schemes for the modified anomalous fractional sub-diffusion equation and the fractional diffusion-wave equation. J. Comput. Phys. **277**, 1–15 (2014)
27. Gao, G.H., Sun, H.W., Sun, Z.Z.: Stability and convergence of finite difference schemes for a class of time-fractional sub-diffusion equations based on certain superconvergence. J. Comput. Phys. **280**, 510–528 (2015)
28. Zhai, S.Y., Feng, X.L.: Investigations on several compact ADI methods for the 2D time fractional diffusion equation. Numer Heat Transfer B **69**, 364–376 (2016)
29. Dimitrov, Y.: Numerical approximations for fractional differential equations. arXiv:1311.3935v1 (2013)
30. Chan, R.H., Jin, X.Q.: An introduction to iterative toeplitz solvers, SIAM (2007)
31. Chan, R.H.: Toeplitz preconditioners for Toeplitz systems with nonnegative generating functions. IMA J. Numer. Anal. **11**, 333–345 (1991)
32. Quarteroni, A., Sacco, R., Saleri, F.: Numerical Mathematics, 2nd ed. Springer (2007)
33. Laub, A.J.: Matrix Analysis for Scientists and Engineers, SIAM (2005)
34. Zeng, F.H., Li, C.P., Liu, F.W., Turner, I.: Numerical algorithms for time-fractional subdiffusion equation with second-order accuracy. SIAM J. Sci. Comput. **37**, A55-A78 (2015)
35. Zhao, X., Sun, Z.Z., Hao, Z.P.: A fourth-order compact ADI scheme for two-dimensional nonlinear space fractional schrödinger equation. SIAM J. Sci. Comput. **36**, A2865-A2886 (2014)
36. Zhai, S.Y., Feng, X.L., He, Y.N.: An unconditionally stable compact ADI method for three-dimensional time-fractional convection-diffusion equation. J. Comput. Phys. **269**, 138-155 (2014)